

# **KAIREI Cruise Report**

## **KR09-16**

### **Studies on the thermal structure and the water distribution in the upper part of the Pacific plate subducting along the Japan Trench**



Japan Trench area

October 30, 2009 – November 12, 2009

Japan Agency for Marine-Earth Science and Technology  
(JAMSTEC)

# Contents

1. Cruise Information	1
2. Researchers	2
3. Observation	3
3.1. Introduction	3
3.2. Summary of the Cruise	5
3.2.1. Research items	5
3.2.2. Cruise schedule and operations	6
3.2.3. Ship track and observation points	8
3.3. Research Objectives	9
3.3.1. Heat flow measurement	9
3.3.2. Natural and controlled source electromagnetic survey	11
3.4. Instruments and Operation Methods	14
3.4.1. Deep-sea heat flow probe	14
3.4.2. Heat flow piston coring system	17
3.4.3. Long-term temperature monitoring systems	19
3.4.4. Physical properties of core samples	22
3.4.5. Ocean-bottom electromagnetometer (OBEM)	22
3.4.6. Kaiko CSEM system	25
3.5. Preliminary Results	30
3.5.1. Heat flow measurement	30
3.5.2. Long-term temperature monitoring	31
3.5.3. Piston core samples	33
3.5.4. Recovery of LT-OBEMs	37
3.5.5. HF-OBEM operation	44
3.5.6. Kaiko CSEM experiment	48
3.5.7. Bathymetry and geophysical survey	53
4. Notice on Using	54
5. Acknowledgements	55
6. References	56
7. Appendices	58
7-1. Cruise Log	58
7-2. Bathymetry Survey Lines	63

# 1. Cruise Information

Cruise number:  
KR09-16

Ship name:  
R/V KAIREI (with ROV KAIKO 7000II)

Title of the cruise:  
2009 Deep Sea Research  
Research cruise with KAIREI and research dives with KAIKO 7000II

Title of proposal:  
S09-64  
Studies on the thermal structure and the water distribution in the upper part of the Pacific plate subducting along the Japan Trench

Cruise period:  
October 30, 2009 – November 12, 2009

Port call:  
2009 Oct. 30 Dept. from Yokosuka (JAMSTEC)  
Nov. 12 Arriv. at Yokosuka (JAMSTEC)

Research area:  
Japan Trench area

Research map:

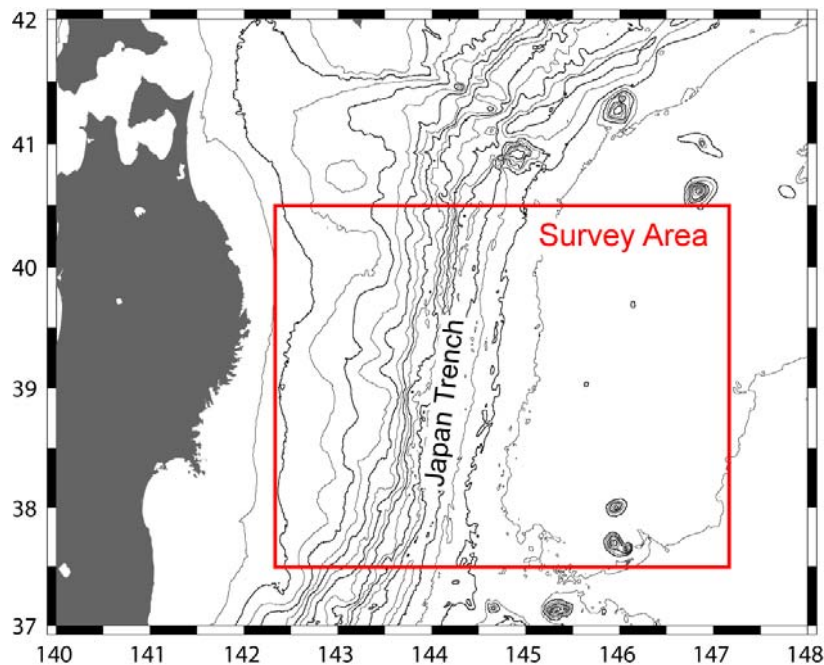


Figure 1-1. Survey area of KR09-16 cruise

Ship track and observation points are shown in 3.2.3.

## 2. Researchers

### Chief Scientist:

Makoto YAMANO Earthquake Research Institute, University of Tokyo

### Science Party:

Makoto YAMANO Earthquake Research Institute, University of Tokyo  
Tada-nori GOTO Graduate School of Engineering, Kyoto University  
Kiyoshi BABA Earthquake Research Institute, University of Tokyo  
Takafumi KASAYA IFREE, JAMSTEC  
Kiichiro KAWAMURA Fukada Geological Institute  
Yoshifumi KAWADA IFREE, JAMSTEC  
Makoto HARADA Institute of Oceanic Research and Development,  
Tokai University  
Xiaobin SHI South China Sea Institute of Oceanology,  
Chinese Academy of Sciences  
Xiaoqiu YANG South China Sea Institute of Oceanology,  
Chinese Academy of Sciences  
Chih-wen CHIANG Graduate School of Engineering, Kyoto University  
Masato YOKOYAMA Graduate School of Life and Environmental Sciences,  
University of Tsukuba  
Koki KAWAMURA Graduate School of Life and Environmental Sciences,  
University of Tsukuba  
Masataka KINOSHITA IFREE, JAMSTEC (shore-based)  
Shusaku GOTO Institute for Geo-Resources and Environment, (shore-based)  
National Institute of Advanced Industrial Science and Technology  
Hideki HAMAMOTO Center for Environmental Science in Saitama (shore-based)  
Tetsuzo SENO Earthquake Research Institute, University of Tokyo (shore-based)  
Toshiya FUJIWARA IFREE, JAMSTEC (shore-based)  
Junji YAMAMOTO Institute for Geothermal Sciences, Kyoto University (shore-based)

### Technical Support Staff

Shinichi HOSOYA Nippon Marine Enterprises, Ltd.  
Ei HATAKEYAMA Marine Works Japan, Ltd.  
Yutaka MATSUURA Marine Works Japan, Ltd.  
Akira SO Marine Works Japan, Ltd.  
Yuji FUWA Marine Works Japan, Ltd.

### 3. Observation

#### 3.1. Introduction

In the Japan Trench subduction zone, an old oceanic plate with an age of over 100 m.y., the Pacific plate, is subducting beneath the northeast Japan arc. Recent studies have revealed that the Pacific plate just before subduction may not be uniformly cold contrary to its old age.

Yamano et al. (2008) conducted heat flow measurements on the seaward slope and the outer rise of the Japan Trench along a parallel of 38°45'N and showed the existence of high heat flow anomalies (Fig. 3.1.1). High heat flow values (70 to 115 mW/m<sup>2</sup>) were obtained at many stations, while values normal for the seafloor age (about 50 mW/m<sup>2</sup>) were also observed at some stations. It suggests that thermal structure of the Pacific plate in this area is not a typical one for old oceanic lithosphere, at least at shallow depths.

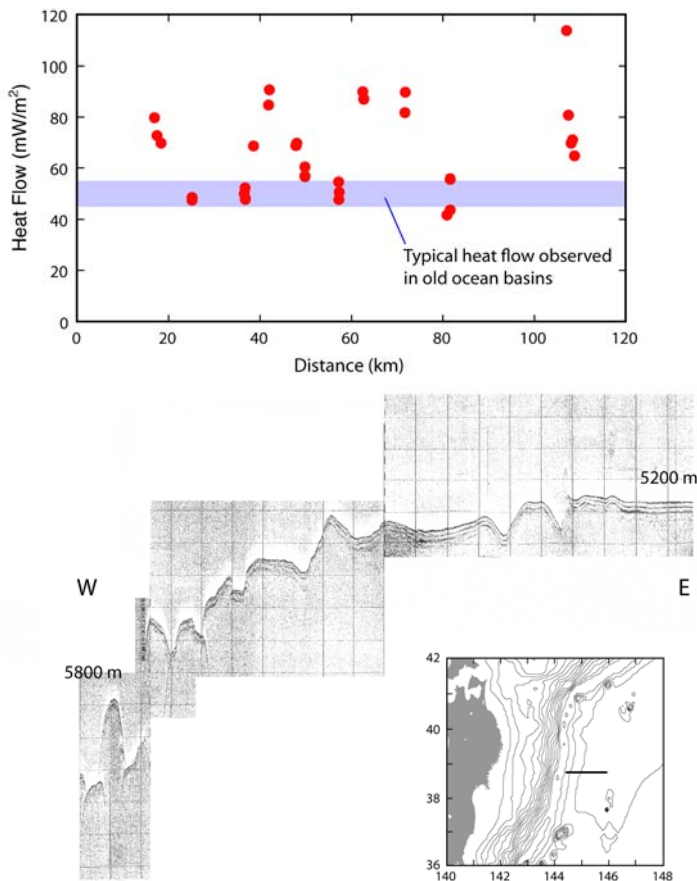


Figure 3.1-1. Heat flow profile on the seaward slope of the Japan Trench along a parallel of 38°45'N projected on a 3.5 kHz subbottom profiler record (Yamano et al., 2008).

Another recent finding is a peculiar type of intra-plate volcanism around the outer rise of the Japan Trench, which is called “petit-spot” (Hirano et al., 2001; 2006). Basaltic rocks with radiometric ages ranging from 4.2 to 8.5 m.y. were collected on the seaward slope of the trench and even younger rocks (younger than 1 m.y.) were found on the eastern edge of the outer rise.

This volcanism might provide a heat source of the observed high heat flow anomalies and exert a significant influence on the thermal structure of the Pacific plate.

Subduction of oceanic plate causes large thrust earthquakes along the interface with the overlying landward plate. The extent of the seismogenic zone of these earthquakes is thought to be controlled mainly by the temperature distribution along the plate interface (e.g., Oleskevich et al., 1999). The existence of water along the plate interface should also play important roles in the stress accumulation and rupture processes in the seismogenic zone. In the Japan Trench subduction zone, the nature of the seismogenic zone, such as seismicity, size of asperities and coupling of the plates, significantly varies along the trench (e.g., Yamanaka and Kikuchi, 2004). Such variations could be related to the temperature structure and water content along the plate interface.

It is therefore important to accurately estimate the temperature structure around the plate interface for studies of seismogenic processes in the Japan Trench subduction zone. We, however, do not have surface heat flow data enough to constrain the thermal model of the subduction zone. It is necessary to conduct more systematic and dense heat flow measurements both on the seaward and landward slopes of the trench..

Results of electromagnetic survey conducted on the landward slope of the Japan Trench show that the subducted oceanic crust has high electrical conductivity and thus contains a large amount of water (Goto et al., 2001), though we do not know where and how the water penetrated into the crust. It is critically important to clarify the penetration process and distribution of the water in the oceanic crust for investigation of the mechanical properties of the plate interface.

In consideration of importance of knowing the temperature and electrical conductivity structures of the subducting Pacific plate, which is mentioned above, we started a research project “Studies on the thermal structure and the water distribution in the upper part of the Pacific plate subducting along the Japan Trench” in 2007, supported by a Grant-in Aid for Scientific Research (19340125) from JSPS. Within the framework of this project, we conducted heat flow measurements and electromagnetic surveys in the Japan Trench area on four cruises (KH-07-3 of R/V Hakuho-maru, KR08-10 of R/V Kairei with ROV Kaiko 7000II, KT-08-25 and KT-09-8 of R/V Tansei-maru. The research plan of this cruise (KR09-16) was made based on the results of the previous four cruises as shown in the following sections and the data we obtained on this cruise will be analyzed and/or synthesized with them.

## **3.2. Summary of the Cruise**

### **3.2.1. Research items**

(1) Heat flow measurement

Heat flow measurement with ordinary deep-sea heat flow probes and stand-alone heat flow meter (SAHF) designed for use in submersible dives.

(2) Long-term temperature monitoring on the seafloor

Long-term monitoring of the bottom water temperature and temperature profile in surface sediment using pop-up type instruments for determination of heat flow in areas with relatively shallow water depths.

(3) Piston core sampling with heat flow measurement (HFPC)

Sampling of surface sediments with a piston corer and heat flow measurement at the same site using temperature sensors mounted on the core barrel.

(4) Ocean-bottom electromagnetic survey

Controlled-source electromagnetic (CSEM) survey with KAIKO 7000II system and magnetotelluric survey with high-frequency ocean-bottom electrometers (HF-OBEMs) and long-term OBEMs (LT-OBEMs).

(5) Bathymetry and geophysical survey

Bathymetry mapping with a multi narrow beam system, gravity measurement, and measurements of total magnetic field and geomagnetic vector.

### 3.2.2. Cruise schedule and operations

Date	Events, Operations
Oct. 30	Leave Yokosuka (JAMSTEC)
Oct. 31	Arrive in the survey area Recovery of two LT-OBEMs (C1 and C4) Deployment of two HF-OBEMs (C2 and C3)
Nov. 1	Recovery of LT-OBEMs (B1) Recovery of pop-up long-term heat flow instrument (PHF01) Heat flow measurement (HF01) Recovery of pop-up water temperature monitoring system (PWT01)
Nov. 2	Recovery of LT-OBEMs (A1) Take refuge from rough sea (Miyako Inlet)
Nov. 3	Transit to the survey area Recovery of pop-up long-term heat flow instrument (PHF02) Heat flow measurement (HF02)
Nov. 4	Bathymetry survey Recovery of LT-OBEMs (B2) Piston core sampling with heat flow measurement (HFPC01) Heat flow measurement (HF03) Transit to Miyako Inlet
Nov. 5	Embarkation and disembarkation of scientists and crew members (Miyako) Sheave exchange (Miyako) Transit to the survey area Attempt to recover pop-up water temperature monitoring system (PWT03) Bathymetry and geophysical survey
Nov. 6	Deployment of HF-OBEM (A5) Controlled-source electromagnetic survey with KAIKO 7000II (Dive #461) Bathymetry and geophysical survey
Nov. 7	Controlled-source electromagnetic survey and core sampling with KAIKO 7000II (Dive #462) Recovery of HF-OBEM (A5) Bathymetry and geophysical survey
Nov. 8	Controlled-source electromagnetic survey with KAIKO 7000II (Dive #463) Recovery of HF-OBEM (C3) Bathymetry and geophysical survey

Nov. 9	Recovery of HF-OBEM (C2) Transit to Kamaishi Inlet Sheave exchange (Kamaishi) Transit to the survey area
Nov. 10	Piston core sampling with heat flow measurement (HFPC02) Leave the survey area
Nov. 11	Transit to Yokosuka Arrive in Tokyo Bay
Nov. 12	Arrive at Yokosuka (JAMSTEC)

Detailed cruise log is given in the Appendices (7-1).

### 3.2.3. Ship track and observation points

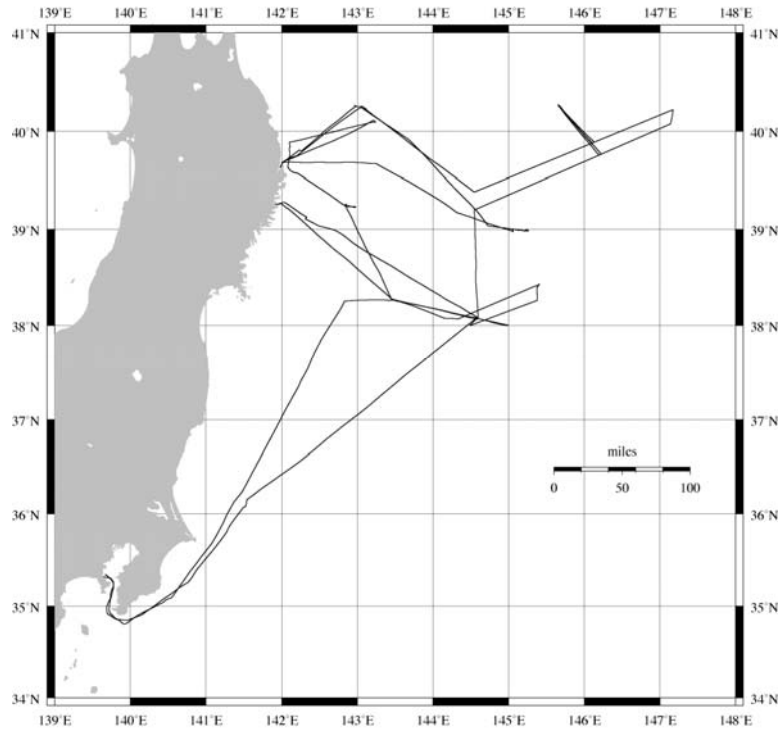


Figure 3.2-1. Ship track of KR09-16 cruise.

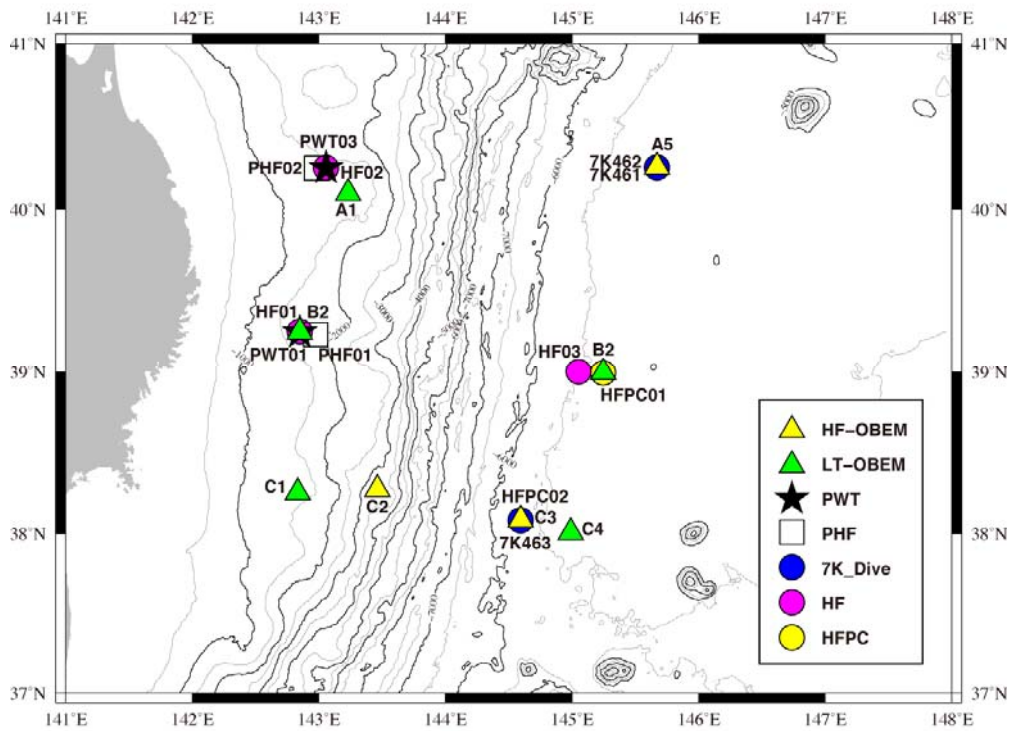


Figure 3.2-2. Measurement and sampling stations on KR09-16 cruise.

### 3.3. Research Objectives

We intend to clarify the temperature structure and the water distribution in the upper part of the Pacific plate subducting beneath the northeast Japan arc through heat flow measurements and electromagnetic surveys in the Japan Trench area. Based on the obtained results, we will investigate intra-plate volcanism on the Pacific plate, heat transfer and water movement in the oceanic crust associated with development of normal faults on the seaward slope of the Japan Trench. We also intend to examine relation between the temperature structure and water distribution along the subducting plate boundary and mechanical properties of the seismogenic zone.

#### 3.3.1. Heat flow measurement

Heat flow values measured on the seaward slope of the Japan Trench along a parallel of 38°45'N are high at some locations and normal for the seafloor age at others (Yamano et al., 2008; Fig. 3.1-1). A possible cause of the spatial variation of heat flow is fluid flow along normal faults developed on the seaward slope of the trench, although no clear correlation between the heat flow distribution and the seafloor topography is recognized. The high average heat flow requires the existence of some heat source in the upper part of the plate. The heat source may be provided by intra-plate (“petit-spot”) volcanism taking place around the outer rise.

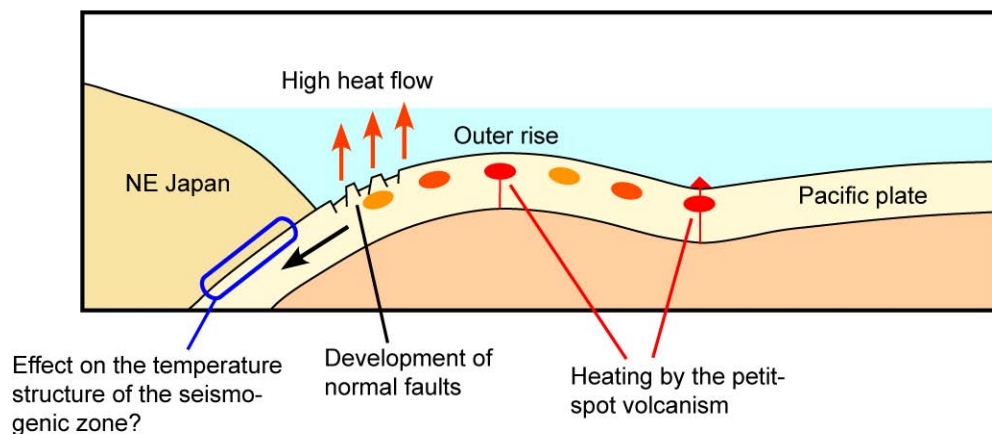


Figure 3.3-1. Schematic model of possible processes giving high heat flow on the seaward slope of the Japan Trench (Yamano et al., 2008).

A qualitative model which may account for the observed heat flow is shown in Fig. 3.3-1. When the Pacific plate reaches the trench outer rise area, melts produced by the petit-spot volcanism repeatedly intrude into the uppermost mantle and/or the lower crust with some eruption at the seafloor, and heat the surroundings. Then development of normal faults in the vicinity of the trench allows fluid flow along the fault zones, which carry heat and focus heat

loss from the layers heated by intrusions. The effective vertical thermal diffusivity may vary from place to place depending on the permeability of fault zones and result in variable heat flow.

The model presented above is rather speculative and needs to be improved through more geophysical and petrological studies, including detailed heat flow surveys. It is necessary to conduct measurements at different latitudes, to make dense measurements around sites with high values, and to investigate relationship between the heat flow distribution and the crustal structure.

The thermal structure of the subducting plate is one of the key factors which control the temperature distribution of the plate interface including the seismogenic zone of large thrust earthquakes. Subduction of the plate, the upper part of which has been anomalously heated, would result in an anomalous temperature structure along the plate interface, affecting mechanical properties of the seismogenic zone.

We chose three lines across the northern Japan Trench (lines A, B, and C in Fig. 3.3-2), along which seismic refraction and reflection surveys were conducted (Tsuru et al., 2000; Ito et al., 2004; Miura et al., 2005), as survey lines for the research project “Studies on the thermal structure and the water distribution in the upper part of the Pacific plate subducting along the Japan Trench” (cf. 3.1). The three lines go through regions with different degrees of seismic coupling along the subduction plate interface (e.g., Yamanaka and Kikuchi, 2004). Comparison of temperature and electrical conductivity structures along these lines will provide information on physical processes in the seismogenic zone.

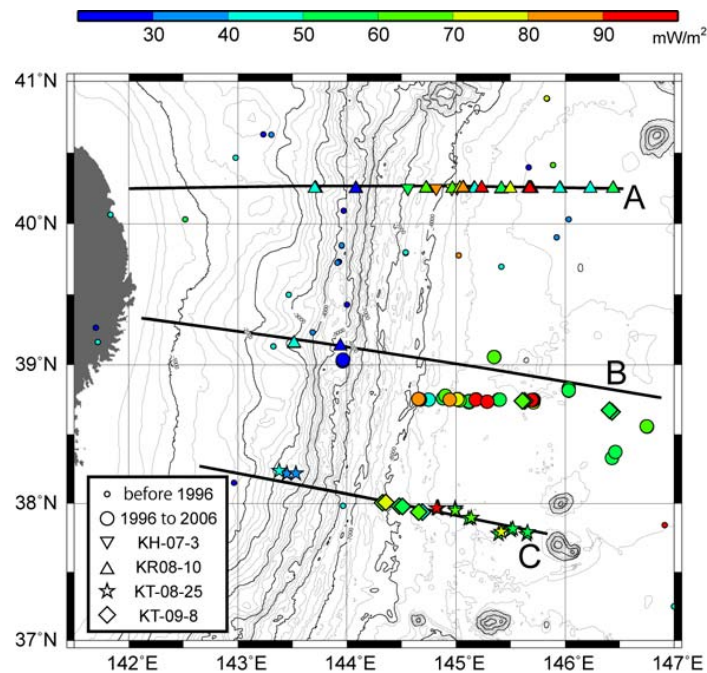


Figure 3.3-2. Heat flow data in the northern Japan Trench area.

Along a parallel of 38°45'N on the seaward side of the Japan Trench, close to the seaward part of the line B, relatively dense heat flow surveys had been made by Yamano et al. (2008). In the project, therefore, we have conducted heat flow measurements mainly along the lines A and C, and the landward part of the line B (Fig. 3.3-2). New data obtained on the previous four cruises (KH-07-3, KR08-10, KT-08-25 and KT-09-8) revealed that heat flow distributions on the seaward slope and outer rise of the trench along the lines A and C is similar to that along 38°45'N (Yamano et al., 2009). High values (higher than 70 mW/m<sup>2</sup>) were measured at many stations, while normal values (about 50 mW/m<sup>2</sup>) were obtained at other stations.

On this cruise, we tried to obtain heat flow data in shallow areas with water depths of less than 2000 m, by combining sediment temperature profiles measured with ordinary deep-sea probe with long-term records of bottom water temperature and temperatures in surface sediment. We also planned to conduct additional measurements on the seaward side in order to obtain heat flow data at OBEM sites and to investigate small-scale variation in the vicinity of specific high anomalies.

### 3.3.2. Natural and controlled source electromagnetic survey

The Pacific plate at the seaward slope of the Japan Trench is very old and should have low heat flow values. However, recent dense heat flow measurements indicate high anomalies seaward of the Japan Trench (Yamano et al. 2008). In order to elucidate the source depth of high heat-flow anomalies, we conduct hybrid marine EM surveys with ocean-bottom electromagnetometers (OBEMs) in this cruise (Fig. 3.3-3).

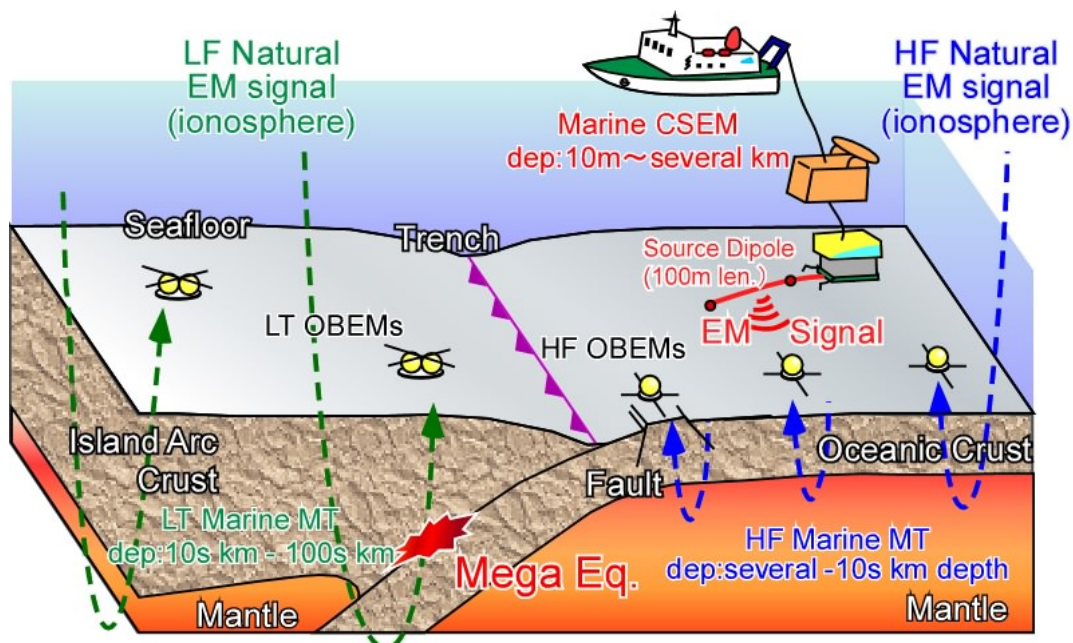


Figure 3.3-3. Basic concept of the hybrid marine EM survey on KR09-16 cruise.

We conduct three different ocean-bottom electromagnetic surveys around the Japan Trench as follows:

- 1) marine controlled-source electromagnetic (CSEM) survey with ROV Kaiko system,
- 2) marine magnetotelluric (MT) survey with short-term or high-frequency OBEMs (HF-OBEM),
- 3) marine MT survey with long-term OBEMs (LT-OBEMs).

Marine CSEM survey will image the electrical conductivity structure near the seafloor with depth of 10 m – several km. We conduct marine CSEM surveys at two sites: the site A5 near high heat-flow anomaly and the site C3 further south from site A5 (Fig. 3.3-4). Marine MT surveys with HF-OBEMs can image the structure of crust and upper mantle with the depth range from several to several 10s km. We deploy three HF-OBEMs around the Japan Trench (sites C2, C3 and A5). This combination of CSEM and MT surveys is effective to discuss the source depth of heat flow anomalies. For example, the oceanic crust with high fluid content and sub-seafloor groundwater circulation can yield both high heat flow and high electrical conductivity anomalies. High temperature zone below the seafloor can also yield high heat flow and conductivity anomalies. CSEM/MT surveys have possibility to detect the source depth of heat flow anomalies.

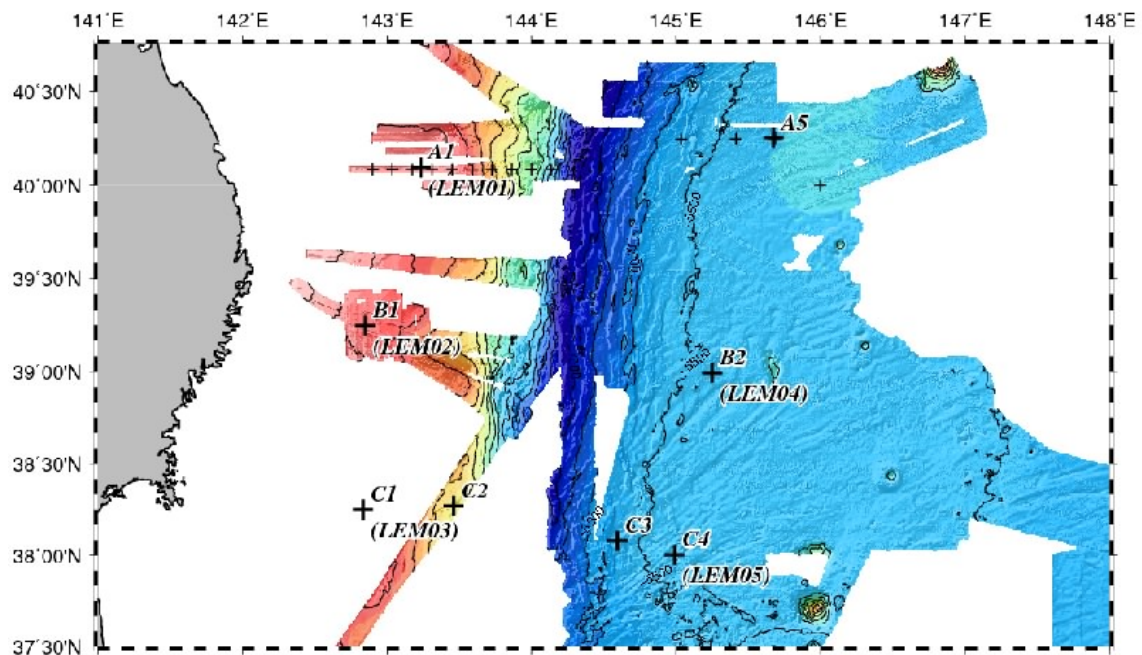


Figure 3.3-4. OBEM site map around the Japan Trench.

CSEM/MT surveys also elucidate how much fluid is included in the oceanic lithosphere of the Pacific plate before its subduction. Fluid in the oceanic lithosphere will be expelled below the Japan Arc after the subduction, relating to the earthquake occurrence near the Japan Trench.

For example, Fujie et al. (2002) carried out seismic reflection survey in the Japan Trench region and found that large amplitude reflected waves generated at the subducting plate boundary were observed at low seismicity region and vice versa. The heterogeneous distribution of seismic reflectors may be attributed to heterogeneous fluid distribution on the plate boundary, and may indicate the role of fluid on the earthquake occurrences. However, we don't know where the fluid is included in the oceanic lithosphere: at a ridge, fracture zones, hot spots or normal faults with horst/graben. Recently, Nakajima and Hasegawa (2006) found that a deep seismically active zone in the subducted Pacific plate corresponds to the elongated low seismic velocity zone, possibly interpreted as an old fracture zone with high fluid content. However, no observed results are reported relating to the fluid content in the oceanic lithosphere before the subduction. In this cruise, we use different types of OBEMs: three HF-OBEMs and five LT-OBEMs. As already described, HF-OBEMs are deployed at sites C2, C3 and A5, and are recovered within this cruise. The LT-OBEMs at sites A1, B1, B2, C1 and C4, deployed at the previous cruises in 2008 and 2009, are recovered at this cruise. With these new dataset, we can compile the existing ocean-bottom EM data since 2000. At the landward slope of the Japan Trench (near site A1), EM data was obtained along a profile with ten HF-OBEMs in 2000. At the seaward slope, western area of site A5, three OBEM/OBEs were deployed and recovered in 2008 (KR08-10 cruise). These previous sites are plotted in Fig. 3.3-4 with smaller marks. Such dense and wide-band MT datasets (especially along profiles at latitude of N40 and N38) give us the electrical conductivity structures of the oceanic lithosphere before and after subduction of the Pacific plate. Such an integrated electrical imaging allows us to discuss how much fluid is included around the normal faults in the horst and graben belt.

Finally, LT-OBEMs give us deeper mantle information. During these several years, many LT-OBEMs have been deployed and recovered around the Japan Trench. The long-term EM fluctuations obtained by the LT-OBEM array allow us to construct a regional 3-D mantle conductivity structure around Japan. Five LT-OBEMs recovered in this cruise are important to image the forearc mantle wedge, the subducting oceanic mantle and oceanic mantle before subduction.

### 3.4. Instruments and Operation Methods

#### 3.4.1. Deep-sea heat flow probe

Heat flow is obtained as the product of the geothermal gradient and the thermal conductivity. We measured the geothermal gradient by penetrating an ordinary deep-sea heat flow probe or a heat flow piston corer (HFPC, cf. 3.4.2) into seafloor sediments.

[Specification of tools]

The deep-sea heat flow probe (Fig. 3.4-1) weighs about 800 kg and has a 4.5 m-long lance, along which seven compact temperature recorders (Miniaturized Temperature Data Logger, ANTARES Datensysteme GmbH; Fig. 3.4-2) are mounted in an outrigger fashion (Ewing type). At some stations, we additionally attached a temperature sensor string containing eight thermistor sensors (in a violin-bow style) to increase the number of temperature measurement points (Fig. 3.4-3). The sensor string is connected to a data logger (Kaiyo Denshi Co., DHF-650), which records temperatures of the sensors and two components of the instrument tilt every 30 sec. The logger sends temperature and tilt data to the surface with acoustic pulses so that we can monitor the status of the probe on the ship.



Figure 3.4-1. Deep-sea heat flow probe.



Figure 3.4-2. ANTARES Miniaturized Temperature Data Logger (MTL).

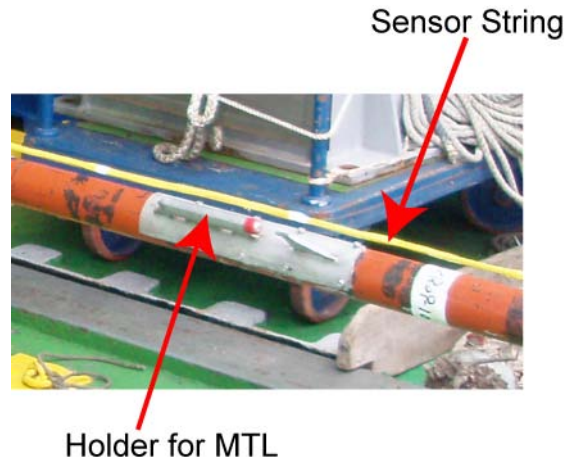


Figure 3.4-3. Thermistor sensor string and holder for ANTARES MTL attached along the lance.

Specifications of the data logger for the heat flow probe and the ANTARES Miniaturized Temperature Data Logger (MTL) are summarized below:

Heat Flow Data Logger DHF-650 (Kaiyo Denshi Co.)

- Pressure case: titanium alloy
- Case length: 725 mm
- Maximum diameter: 145 mm
- Pressure rating: 7000 m water depth
- Number of temperature channels: 9
- Temperature resolution: 1mK
- Tilt: two-axis, 0 to  $\pm 45^\circ$
- Data-cycle interval: 30 sec
- Pinger frequency: 15.0 kHz (or 12.0 kHz)

Miniaturized Temperature Data Logger (ANTARES Datensysteme GmbH)

- Pressure case: stainless steel
- Case length: 160 mm
- Diameter: 15 mm
- Pressure rating: 6000 m water depth
- Number of temperature channel: 1
- Temperature resolution: 1.2 mK at 20°C, 0.75 mK at 1°C
- Sample rate: variable from 1 sec to 255 min.

[Operations]

A 15 m long nylon rope was inserted between the heat flow probe and the winch wire rope in order not to kink the wire rope during probe penetrations. An acoustic transponder and a

pinger were attached 40 m above the probe for precise determination of the position of the probe and the distance from the seafloor (Fig. 3.4-4).

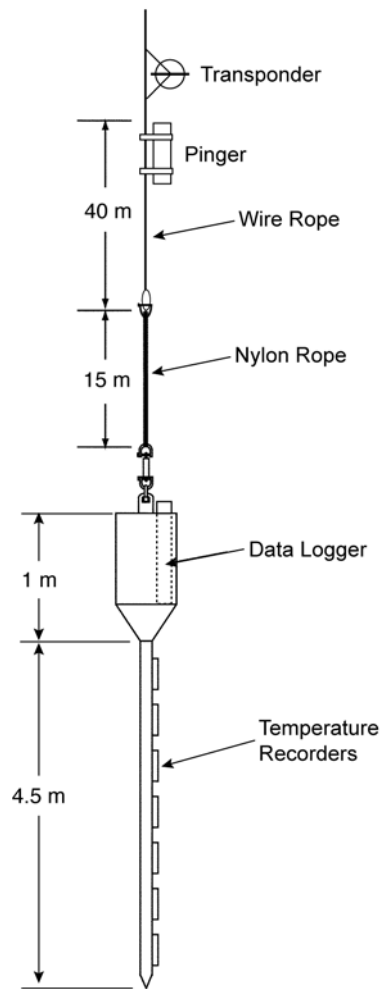


Figure 3.4-4. Configuration of the heat flow measurement system using a deep-sea probe.

Multi-penetration heat-flow measurement operations were conducted following the procedures described below.

1. Measure water temperature about 30 m above the sea floor for calibration of temperature sensors.
2. Lower the probe at a speed of about 1 m/sec until it penetrates into the sediment.
3. Measure temperatures in the sediment for about 20 min. Monitor the wire tension and pay out the wire when necessary to keep the probe stable.
4. Pull out the probe and move to the next station.

### 3.4.2. Heat flow piston coring system

[Specification of tools]

During this cruise, sediment core samples were taken with the heat flow piston coring system (HFPC) (Fig. 3.4-5). This coring system was used for combined operation of measuring heat flow and recovering sediments. The general outline of the system is shown in Fig. 3.4-6.

A stainless steel barrel was attached to a piston core head of 800 kg weight. The core head has a space for mounting the heat flow data logger to record the temperatures of thermistor sensors mounted along the barrel. On this cruise, seven ANTARES MTLs (cf. 3.4.1) were mounted helically on the outside of barrel, between the base of the weight stand and the core catcher bit. A transponder was mounted on the winch wire to obtain the depth and position of this equipment. A pinger was also mounted on the winch wire to obtain the altitude from sea floor. The stainless steel barrel with this system is 4 m in length and liner is used for recovering sediments. The balance and pilot corer are the same as ones for ordinary piston core systems. 24mm nylon rope was placed between the balance and winch wire for additional wire out and/or increased tension after hitting sea bottom. Because the system must be kept in the sediment for 15 to 20 minutes to obtain stable temperature, additional wire out is necessary for avoiding pulling the barrel out of the sea floor by either heaving or drifting of the ship during the measurement.



Figure 3.4-5. HFPC with compact temperature data loggers (MTLs).

[Operations]

#### Preparation for the piston coring

After barrels are attached to the head (weight stand), the main wire is connected, through the barrel, to the piston at the bottom of the barrel. The core catcher and bit are then attached. The balance is connected to the end of the main wire. The entire assemblage is carried under the A-frame using a cart and is lifted over the edge of the deck by the winch. A-frame and

capstan winches, the pilot core and its wire are then connected to the balance. The system is then lowered through the water to the sea floor.

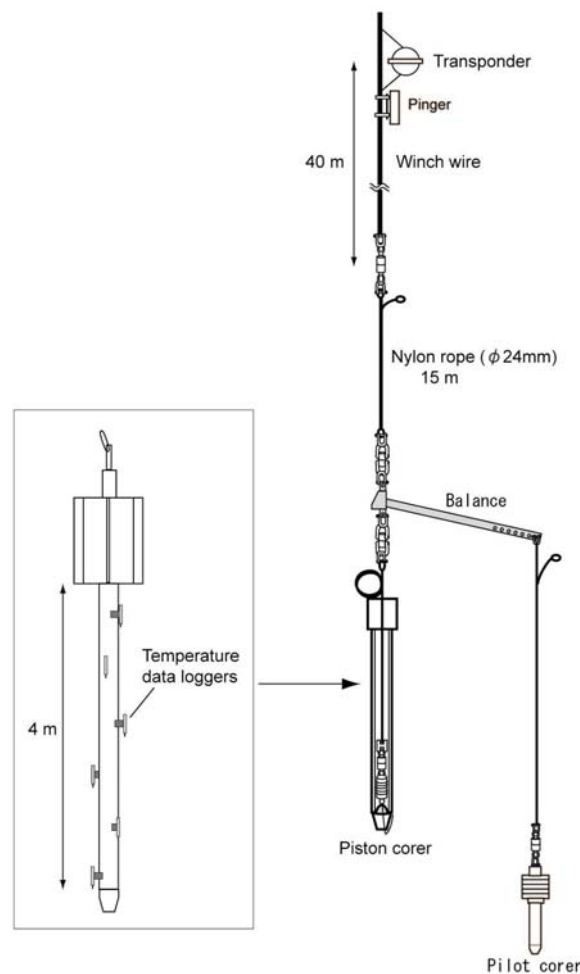


Figure 3.4-6. Configuration of the heat flow piston coring (HFPC) system.

#### Hit the bottom and off the bottom

The piston core system starts lowering at a winch speed of 20 m/min, which is gradually increasing to a maximum 60 m/min. The piston core is stopped at a depth about 50 m above the sea floor for 5 minutes to reduce any pendulum motion and to calibrate the temperature sensors on the outside of barrel.

After 5 minutes, the wire is lowered at a speed of about 20m/min., at the same time carefully watching the pen recorder of the strain gauge tension meter. When the piston core hit the bottom the tension will abruptly decrease by the amount of the piston core weight. Therefore, it is easy to detect the bottom hit.

After the recognition of hit the bottom, add 5m to wire out, stopped and keep the position for 15~20 minutes. And then, rewinding of the wire is started at a dead slow speed (~20 m/min.), until the tension gauge indicate that the core has lifted off the bottom. The tension

meter shows a small increase in tension when the core is being pulled out of the sea floor and then a steady value. After we can recognize absolutely that the piston core is above the sea floor, the winch to keep speed is increased to 60m/min., and then gradually to maximum speed.

### 3.4.3. Long-term temperature monitoring systems

For heat flow measurement at stations with water depths less than 2000 m, we used two types of long-term temperature monitoring systems.

[Pop-up heat flow instrument (PHF)]

We developed pop-up type heat flow probes that can record temperatures in the surface sediment for over one year. Long-term sediment temperature records up to about 400 days have been obtained with these instruments at ten stations in shallow sea areas off Shikoku and off the Ki-i Peninsula. At eight stations where temperature records longer than 220 days were obtained, we could determine the temperature gradient and heat flow by removing the effect of the bottom water temperature variation from the raw temperature data (Hamamoto et al., 2005).

On KR09-16 cruise, we recovered two pop-up heat flow instruments (termed PHFs below; Fig. 3.4-7). The basic configuration and specification of the two instruments are essentially the same. Main components of PHF are a recording unit, a temperature probe and a weight (Fig. 3.4-8). The temperature probe is 2 m long and has six or seven temperature sensors set at even intervals. The recording unit records the measurement date and time, temperatures, and two-axis instrument tilts. The temperature resolution is 1 mK. A small water temperature recorder (NWT-DN, Nichiyu Giken Kogyo Co.) is attached to the main frame for monitoring the bottom water temperature. After recording the sediment temperatures, the PHF releases the weight and temperature probe responding to an acoustic command, and the recording unit pops up and can be recovered with a surface ship.

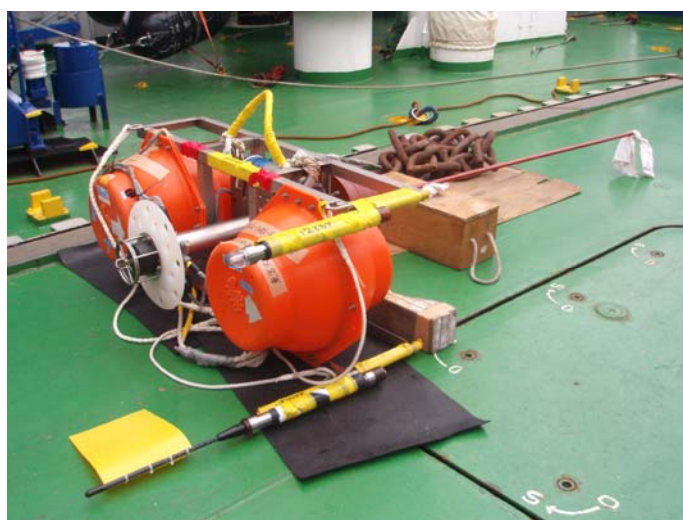


Figure 3.4-7. Pop-up heat flow instrument (PHF) lying on the deck.

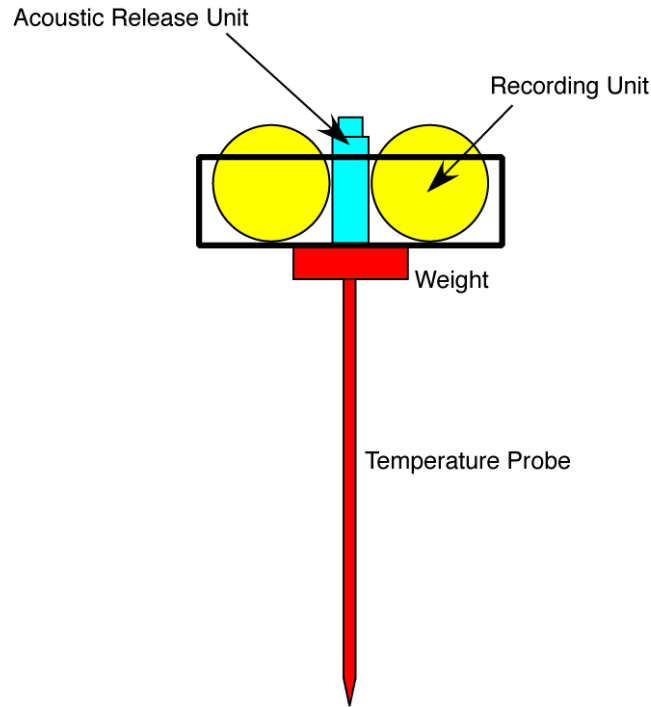


Figure 3.4-8. Schematic configuration of PHF.

Specifications of the water temperature recorder (NWT-DN) are summarized below.

Pressure case	titanium alloy
Case length	212 mm
Diameter	41 mm
Pressure rating	6000 m water depth
Number of temperature channel	1
Temperature resolution	1 mK
Sample rate	variable from 2 sec to 1 day

[Pop-up water temperature measurement system (PWT)]

Heat flow data in shallow sea areas can be obtained through long-term temperature monitoring with PHFs. It is not easy, however, to conduct measurements with PHFs at many stations, since the monitoring period needs to be quite long, about one year, and the instruments are relatively expensive. If we obtain bottom water temperature records at additional stations, we may be able to clarify the general pattern and features of bottom water temperature variations in the study area. Such information will be helpful in determination of appropriate length of the monitoring period for PHFs. Moreover, it is possible to determine heat flow by analyzing the temperature profile measured with ordinary deep-sea probes in combination with the preceding bottom water temperature records.

We have been using a pop-up water temperature measurement system (termed PWT below)

in order to obtain long-term bottom water temperature records (Fig. 3.4-9). PWT consists of an acoustic releaser, weights, floats (glass spheres), and a small water temperature recorder (NWT-DN) (Fig. 3.4-10). For deployment, the whole system is released at the sea surface and it sinks freely down to the sea floor. The system is recovered by activating the acoustic releaser with a command sent from a surface ship.



Figure. 3.4-9. Pop-up water temperature measurement system (PWT).

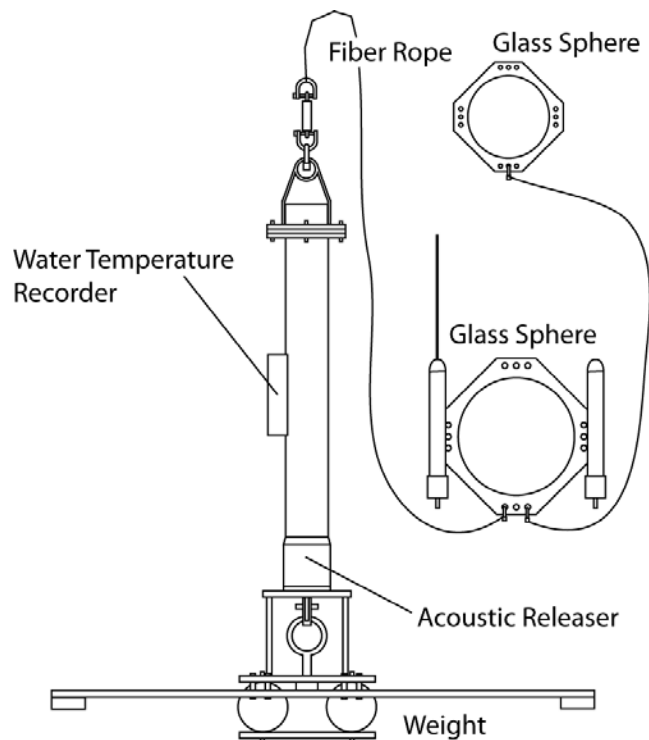


Figure 3.4-10. Schematic drawing of PWT.

#### 3.4.4. Physical properties of core samples

[Thermal conductivity]

We need to know thermal conductivity of surface sediments in order to obtain heat flow values. Thermal conductivity of piston core samples was measured using two different types of line-source commercial devices. One is KD2 Pro (Decagon Devices) with a full-space type needle probe (von Herzen and Maxwell, 1959). The probe was inserted into whole-round core samples. The other is QTM-500 (Kyoto Electronics Manufacturing Co.) with a half-space type box probe (Sass et al., 1984). Measurements with this instrument were made on split core samples.

[Shear strength]

In order to understand shear strengths of core samples under the undrainage and unconsolidation (UU) conditions, we conducted vane shear test. The shear strength is measured using four-wing-bearing torque driver of 2 cm in height and 1 cm in width. The measurement procedure is as follows; 1) the whole wings of the torque driver are penetrated directly into the splitting surface of the working half after cube sampling, 2) the torque driver is rotated slowly, 3) the torque force is recorded at 1 second interval. Each test was done for approximately 20 seconds. If the sediment samples were too hard to measure, the penetration depth of the wings was changed from 2 cm to 1 cm, and measured again for 20 seconds at new surface.

The shear strength is calculated by the shear friction working during rotation of the driver. According to the vane rotation length, it is calculated the one unit on the driver is 4.54 kPa as below calculation.

$$C = \frac{M_{t\max}}{\pi D^2 \left( \frac{H}{2} + \frac{D}{6} \right)}$$

where  $C$  is the shear strength ( $\text{kg}/\text{cm}^2$ ),  $M_{t\max}$  is the torque moment ( $\text{kg cm}$ ),  $H$  is the wing height ( $\text{cm}$ ), and  $D$  is the total wing width ( $\text{cm}$ ).

#### 3.4.5. Ocean-bottom electromagnetometer (OBEM)

[HF-OBEM]

The OBEM system with a high sampling rate was designed to investigate the crustal and mantle structure. This system consists of one 17-inch glass sphere, and then a high-accuracy fluxgate magnetometer is mounted outside the glass sphere (Fig. 3.4-11). Concepts of our developed OBEM system are miniaturization, a high sampling rate, easy assembly and recovery operations, and low costs of construction and operation. It has a folding-arm system to facilitate assembly and recovery operations (Kasaya et al., 2006; Kasaya and Goto, 2009).

Figure 3.4-12 shows the schematic diagram of the arm-folding system. For measuring the electric field, we used Ag-AgCl electrode mounted at the toe of each electrode arm.

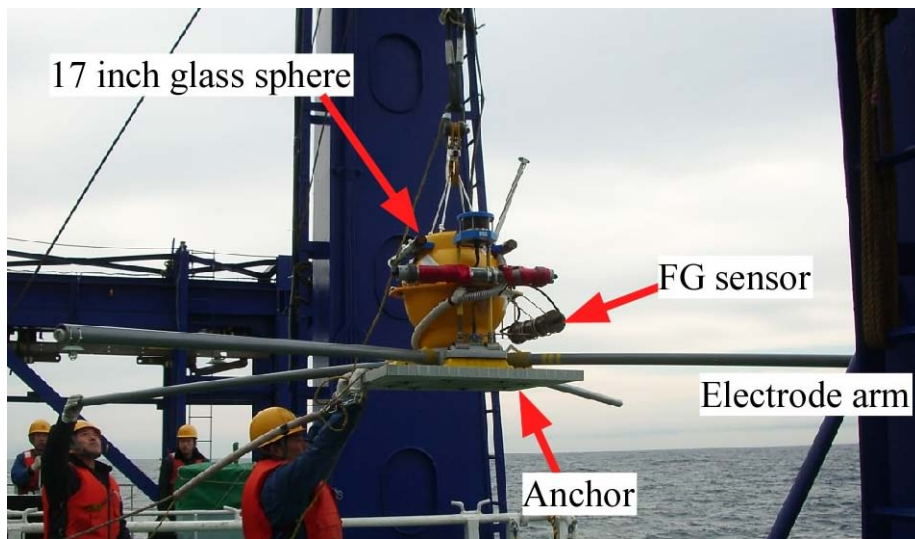


Figure 3.4-11. Photo of a small OBEM system.

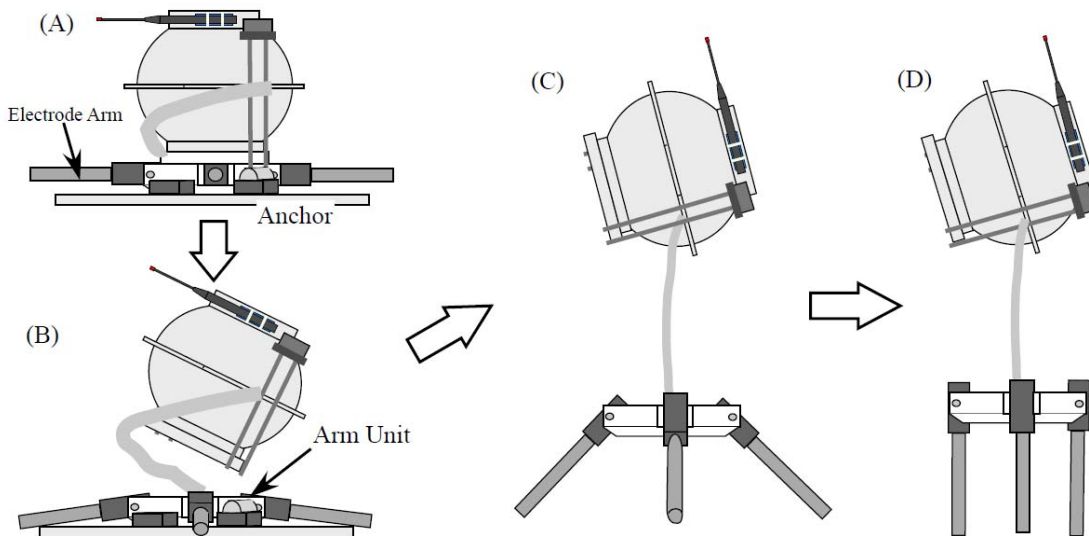


Figure 3.4-12. Schematic diagram of the arm-folding system. After starting to pop up, the arm unit is picked up as the sphere ascends.

Electric circuit used for each system is contained in the pressure glass spheres. The fluxgate magnetometer of the OBEM system is mounted outside the glass sphere (Fig. 3.4-11). The salient characteristic of our system is its arm-folding mechanism, which facilitates and simplifies our onboard operations. We used an acoustic release system that had been already

used by JAMSTEC for Ocean Bottom Seismography (OBS). Therefore, this acoustic system can communicate with the Kairei's SSBL system and it is easy for us to detect its position in the sea or on the seafloor.

Clock synchronization before deployment and calibration after recovery are important. This OBEM system can synchronize to the laptop PC using USB communication. To synchronize the laptop PC to GPS clock, we developed the portable NTP server unit (Fig. 3.4-13).



Figure 3.4-13. Photo of the developed NTP server unit.

#### [LT-OBEM]

The long-term OBEMs (LT-OBEMs) are made by Tierra Technica, which can measure time variations of three components of magnetic field, horizontal electric field, the instrumental tilts, and temperature. The resolutions are 0.01 nT for flux-gate magnetometer, 0.305  $\mu$  V for voltmeter, 0.00026 degrees for tiltmeter, and 0.01° C for thermometer. There are two types of instrumental design (Fig. 3.4-14 and Table 3.4-1). Type 1 LT-OBEM is equipped with three glass spheres on an aluminum frame, housing Benthos acoustic transponder, the electromagnetometer, and a Lithium battery pack for the electromagnetometer, respectively. Type 2 LT-OBEM is an improved version of type 1, which is equipped with two glass spheres on a titanium or aluminum frame. An acoustic transponder and the battery pack are put together in one glass sphere. We have one type-1 LT-OBEM (TT4) and four type-2 LT-OBEMs (TT1, ERI1, ERI2, and ERI12). A radio beacon, a flash light, and a catching buoy for easy recovery are mounted on all LT-OBEMs. For electric field measurements, Ag-AgCl

equilibrium electrodes made by Clover Tech. were utilized. The electrodes were monitored their self potentials in laboratory in advance of the seafloor observation and pairs that the coherence is high enough were selected, in order to reduce the noise due to the voltage drift of electrodes themselves.



Figure 3.4-14. Type 1 LT-OBEM (left) and Type 2 LT-OBEM (right).

Table 3.4-1. Specification of LT-OBEMs

OBEM ID	Type	Dipole length (m)	Acoustic code	Beacon frequency
TT1	2 (Titanium frame)	5.41(NS) / 5.41 (EW)	4A-1 (KDC)	43.528 MHz (JS190)
TT4	1 (Aluminum frame)	5.24 / 5.22	C (Benthos*)	43.528 MHz (JS1086)
ER11	2 (Titanium frame)	5.37 / 5.37	1D-1 (KDC)	159.20 MHz
ER12	2 (Aluminum frame)	5.39 / 5.39	1E-1 (KDC)	159.30 MHz
ER112	2 (Aluminum frame)	5.38 / 5.38	3E-1 (KDC)	159.25 MHz

\* Tx: 11.0 kHz, Rx: 10.0 kHz

### 3.4.6. Kaiko CSEM system

In this cruise, we used a new controlled-source electromagnetic (CSEM) system operated by the ROV “Kaiko 7000II”. The schematic explanation of the system is shown in Fig. 3.4-15. The detail of the system is explained in the following photos. During Dive #461 - #463, the transmitter on the Kaiko vehicle sends the artificially controlled electric current (with squared waves) using a 20m-dipole cable. An OBEM (ocean bottom electromagnetometer) receive the EM signal, and then we can estimate the apparent resistivity at the seafloor. Since the seawater conductivity is measurable with the CTD sensor attached to the Kaiko vehicle, we can obtain the electrical conductivity distribtution below the seafloor. Also, the electrical potential field generated by artificial current can be measured by the ROV itself using many electrodes attached to both the cable and the ROV frame. Those short-range received values can be used for imaging the shallow sediments just below the seafloor.

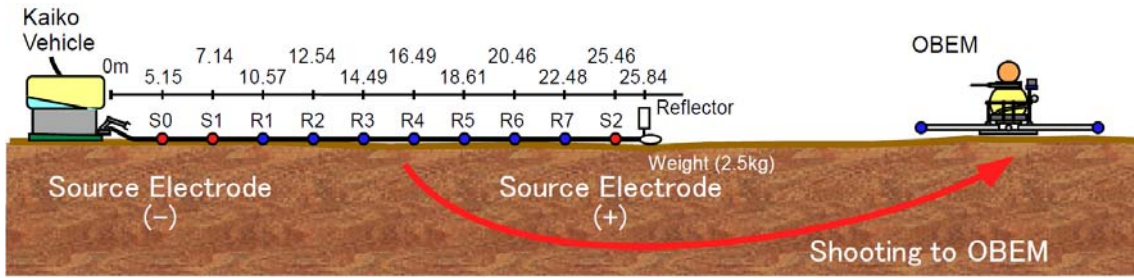


Figure 3.4-15. Concept of the Kaiko CSEM experiment. Electrode locations, actually adopted in this experiment are also shown. Red circles: source electrodes, blue circles: potential electrodes.

Unfortunately, the transmitter had a problem when we tested it onboard before the first dive (#461). Due to the heat generated by the transmitter itself, a circuit for transmitter was partly broken. We refined the problem, but we forgave to switch the source electrode and fixed (S0=negative, S1=not used, and S2=positive electrodes, respectively).

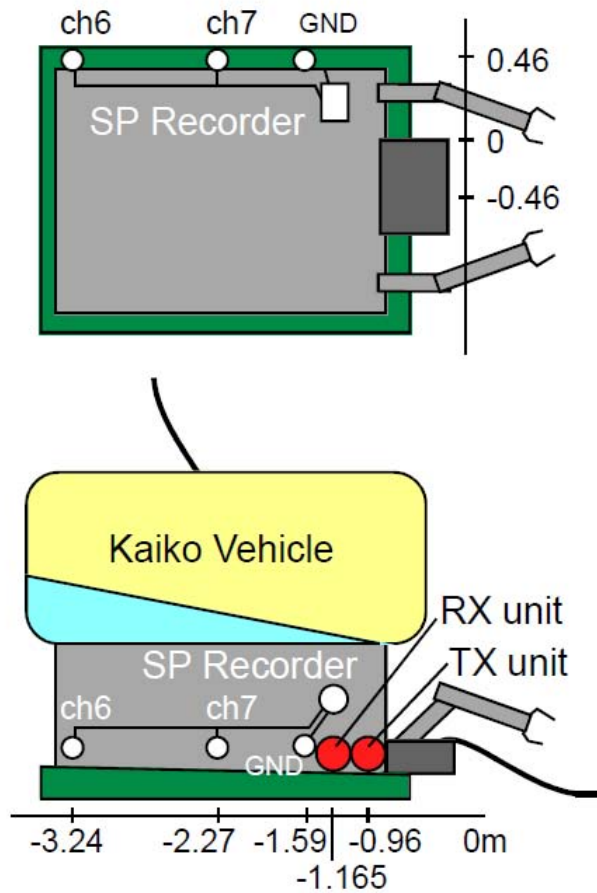


Figure 3.4-16. Close-up of the several units and sensors on the ROV Kaiko 7000II.

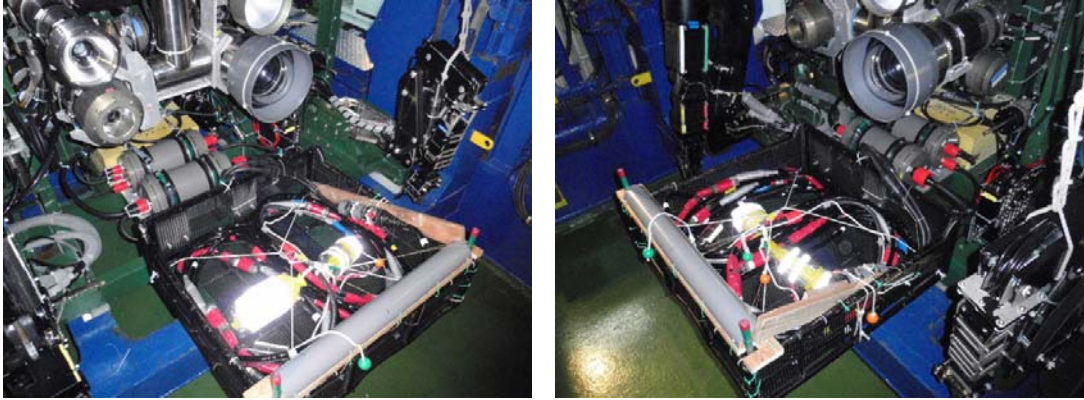


Figure 3.4-17. Payload of the ROV Kaiko 7000II (STBD and PORT sides).



Figure 3.4-18. Transmitter (TX) and receiver (RX) unit.

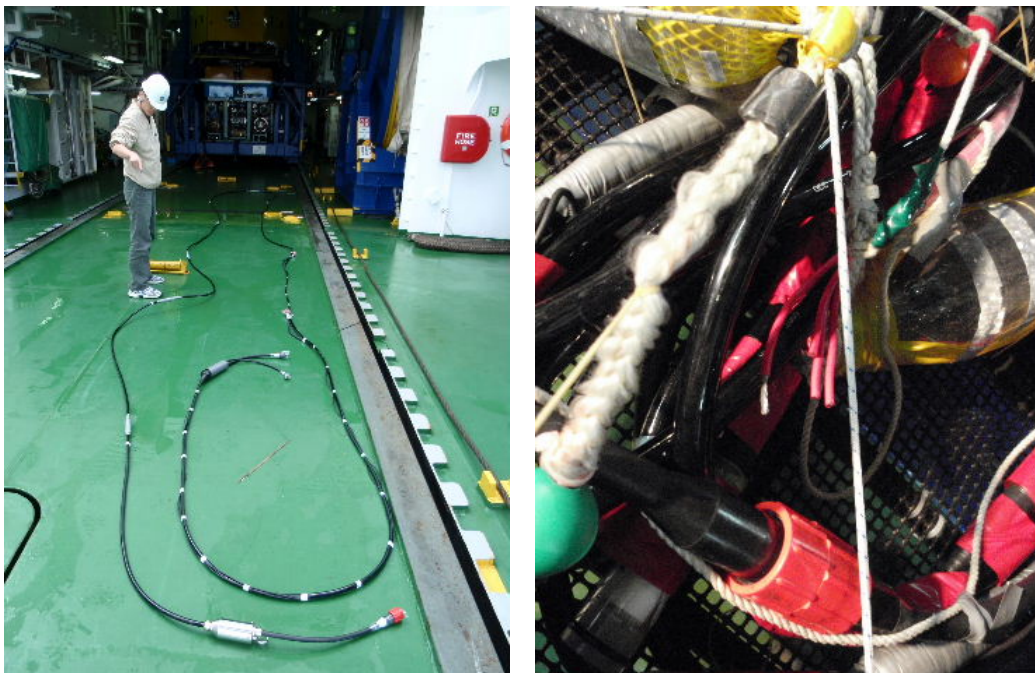


Figure 3.4-19. 20m-length cable (left) and a source electrode (S2: right).



Figure 3.4-20. Source Electrode (left) and cable termination (right).



Figure 3.4-21. Receiver electrode (Ag-AgCl).

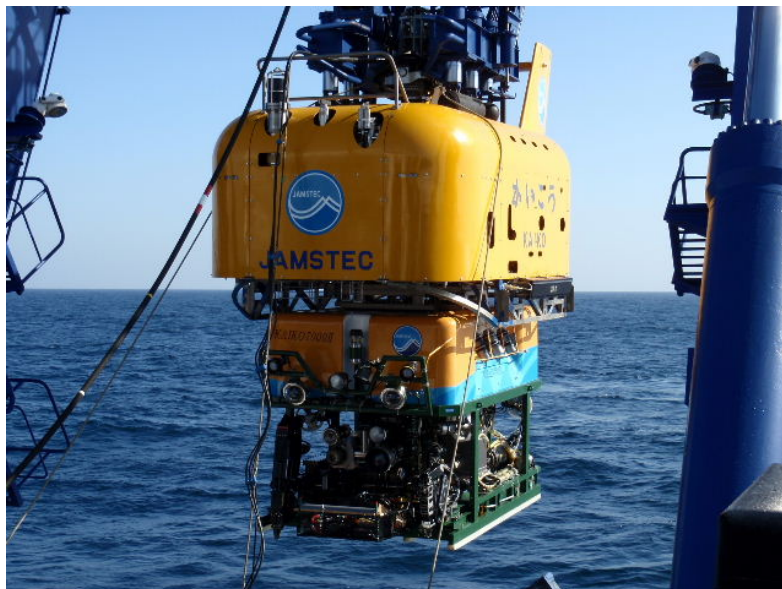


Figure 3.4-22. ROV Kaiko 7000II before the diving (#461).

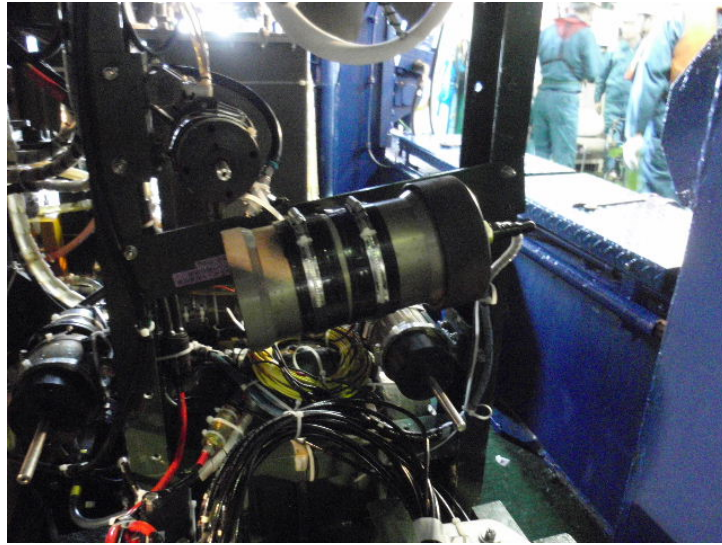


Figure 3.4-23. SP recorder (see Fig. 3.4-16).

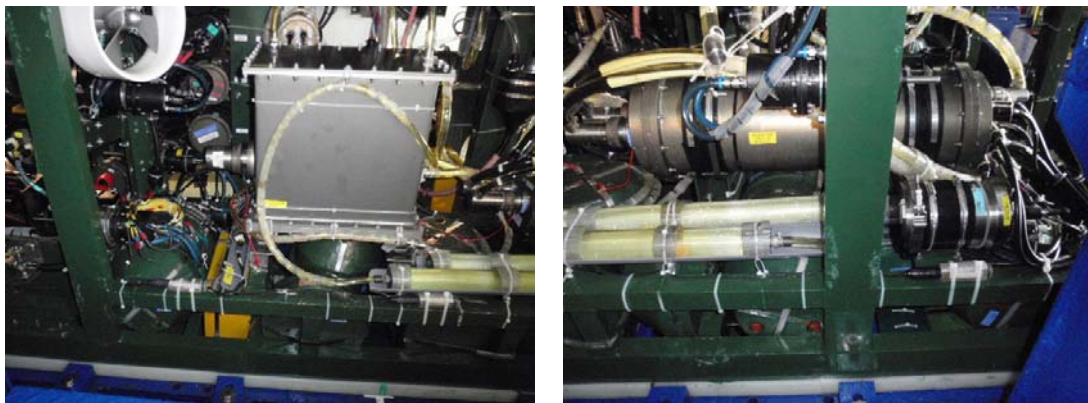


Figure 3.4-24. Ag-AgCl electrodes for the SP recorder (see Fig. 3.4-16).

### 3.5. Preliminary Results

#### 3.5.1. Heat flow measurement

We carried out heat flow measurements at three sites with the deep-sea heat flow probe and at two sites with the HFPC (Table 3.5-1). At all the sites with the deep-sea heat flow probe, multiple penetrations were attempted for examining local variability of heat flow. The coordinates of the stations listed in Table 3.5-1 are the positions of the transponder attached just above the probe or HFPC determined with the SSBL system of the ship, though the position of the ship is shown for HF03 because the transponder did not work during the measurements at this site. The water depth in the table is the depth right below the ship and may be slightly different from the depth at the station.

Sites HF03 and HFPC01 are located on the seaward slope of the Japan Trench at around 39°N along the line B (cf. Fig. 3.3-2). Site HFPC02 is also on the seaward slope along the line C. HFPC01 and HFPC02 are at about the same location as OBEM sites B2 and C3, respectively. Full penetration of the probe could not be attained at HF03, which is probably due to a thick volcanic ash layer.

Table 3.5-1. Results of heat flow measurements

Date	Station	Latitude (N)	Longitude (E)	Depth (m)	N
Deep-sea heat flow probe					
Nov. 1	HF01A	39°15.10'	142°50.97'	1695	6
	B	39°15.11'	142°50.95'	1695	6
	C	39°15.10'	142°50.98'	1695	6
Nov. 3	HF02A	40°15.08'	143°03.39'	1420	5
	B	40°15.09'	143°03.39'	1420	5
	C	40°15.09'	143°03.42'	1425	5
Nov. 4	HF03A	†39°00.09'	†145°03.21'	5510	5
	B	†39°00.10'	†145°03.21'	5505	5
HFPC					
Nov. 4	HFPC01	38°59.64'	145°14.91'	5405	6
Nov.10	HFPC02	38°04.90'	144°35.61'	5750	7

N: number of temperature sensors used to obtain temperature profile in sediment.

†: position of the ship.

Sites HF01 and HF02 are located on the landward side of the trench along the lines B and A. Full penetration of the probe was attained. These sites are in relatively shallow sea areas with water depths of less than 2000 m and the measured temperature profiles must be analyzed with long-term records of bottom water and sediment temperatures. Sites HF01 and HF02 are in the vicinity of the long-term temperature monitoring stations PWT01 and PHF02, respectively (cf. 3.5.2).

Heat flow values will be obtained by combining the measured temperature profiles with thermal conductivity of surface sediment. Thermal conductivity at each site needs to be estimated from the values measured on piston core samples (cf. 3.5.3) and the existing data at nearby stations.

### **3.5.2. Long-term temperature monitoring**

We recovered two pop-up heat flow instruments (PHFs; cf. 3.4.3), which were deployed on KR08-10 cruise for obtaining long-term records of temperature profiles in surface sediment (PHF01 and PHF02 in Table 3.5-2; Fig. 3.5-1). The instruments have six or seven temperature sensors in 2-m long probes and the sampling interval was 20 min. The sediment temperature records collected by both instruments are of good quality, though the data in the last 44 days are missing at PHF01 because of a shortage of memory capacity. Analysis of these temperature records will give reliable heat flow corrected for influence of bottom water temperature variation.



Figure 3.5-1. Recovery of a pop-up heat flow instrument (PHF).

Water temperature recorders (NWT-DN) attached to the frames of the PHFs yielded records of bottom water temperature at the two stations (Fig. 3.5-2). These records can be used for analysis of the temperature profiles measured with the deep-sea heat flow probe at nearby stations.

We also attempted to recover two pop-up water temperature measurement system (PWTs; cf. 3.4.3) deployed during KR-08-10 cruise (PWT01 and PWT02 in Table 3.5-2). One of them (PWT01) was successfully recovered, but the other (PWT03) did not respond to acoustic commands from the ship and did not pop up.

Bottom water temperature records obtained at PHF01, PHF02 and PWT01 are plotted in Figure 3.5-2. The temperature variation at PWT01 is quite similar to the one at PHF01, about 10 km to the east of PWT01. It is interesting that the temperature variation at PHF02, over 100 km away from PWT01 and PHF01, still shows some common features.

Table 3.5-2. Recovery of long-term temperature monitoring instruments

Station	Deployment	Recovery	Coordinates	Water depth (m)
PHF01	Aug. 26, 2008	Nov. 1, 2009	39°14.02'N, 142°58.50'E	1830
PHF02	Aug. 30, 2008	Nov. 3, 2009	40°15.07'N, 142°58.97'E	1420
PWT01	Aug. 26, 2008	Nov. 1, 2009	39°14.89'N, 142°51.11'E	1710
PWT03	Aug. 31, 2008	Failed	40°15.07'N, 143°03.55'E	1420

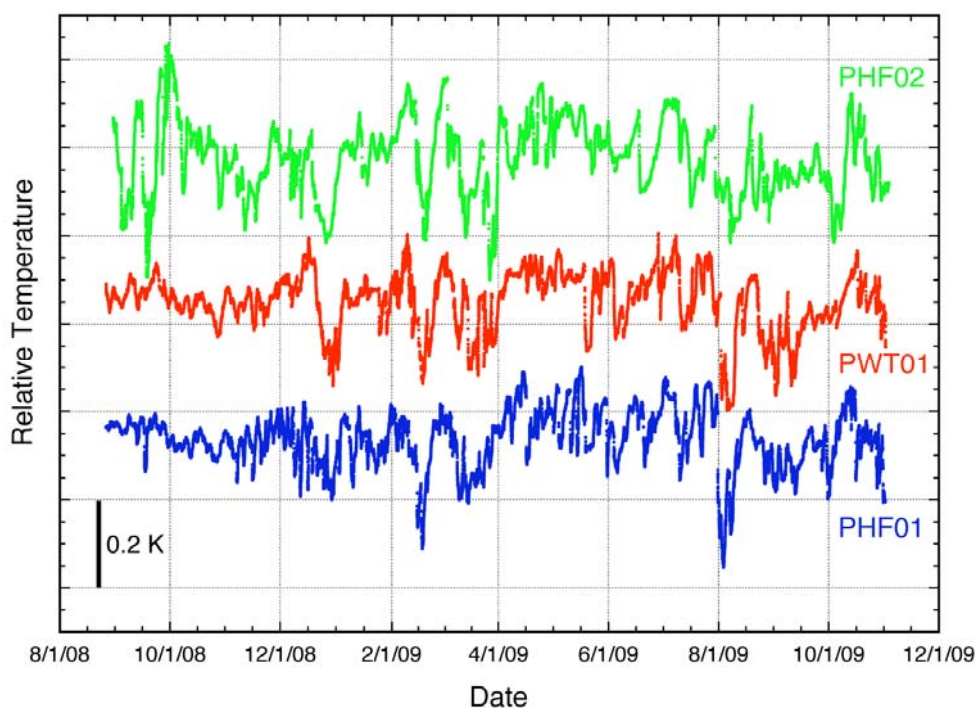


Figure 3.5-2. Bottom water temperature records at PHF01, PWT01, and PHF02.

### 3.5.3. Piston core samples

Two piston core samples were collected at sites off Miyako, northeast Japan using a 4-m-piston-corer system operated by Marine Works Japan Co. Ltd. The piston corer system has a pilot corer, so that a piston core sample and a pilot core sample were collected at one coring site. Seven temperature recorders (ANTARES MTL: cf. 3.4.1) for heat flow measurement were attached along the core barrel of the piston corer to be a heat-flow piston corer (hereafter HFPC). Sample names of piston cores and pilot cores are HFPC (01, 02) and HFPL (01, 02), respectively.

Furthermore, one MBARI type core was collected at a site off Hachinohe using ROV Kaiko 7000II. The locality of these cores is shown in Figure 3.5-3 and the lithological units are summarized in Figure 3.5-4.

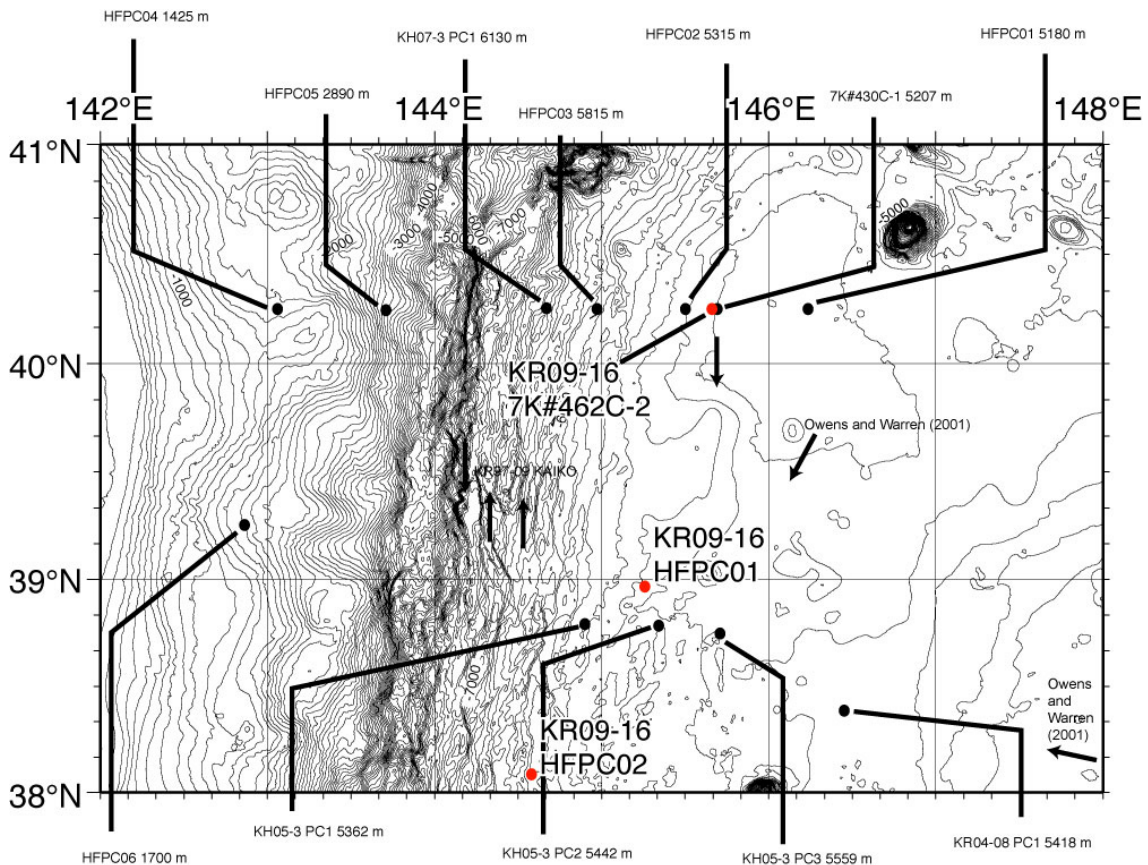


Figure 3.5-3. Coring sites.

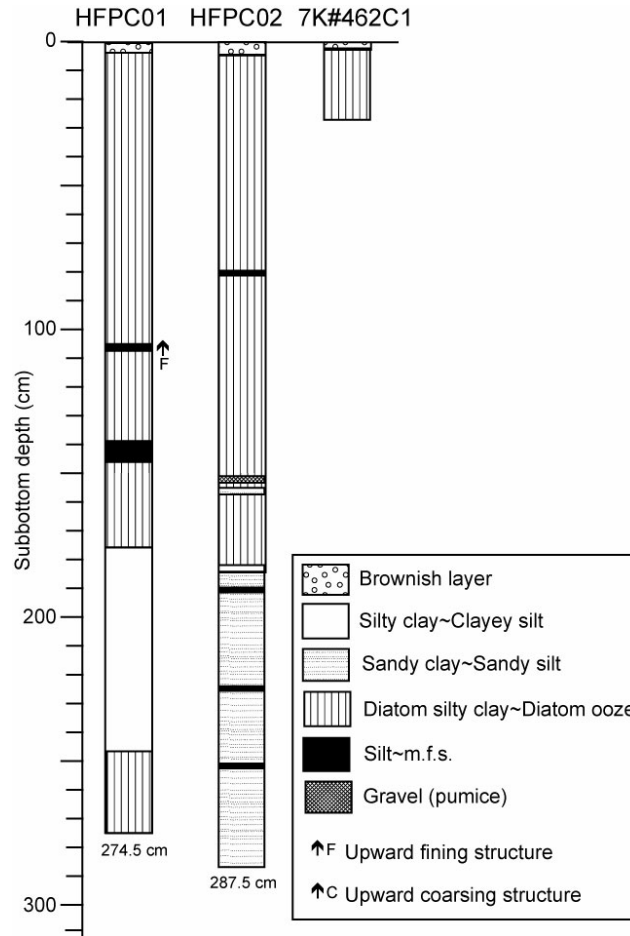


Figure 3.5-4. Lithological units of the piston cores in KR09-16.

The piston core and MBARI core samples were processed as follows;

- 1) Cut the whole core by 1 m section.
- 2) Measure thermal conductivity using a needle probe (see 3.4.4).
- 3) Split the whole core into working half and archive half.
- 4) Measure thermal conductivity of the archive half using a QTM instrument (see 3.4.4).
- 5) Describe the working half by naked eyes and smear slides.
- 6) Take photographs of the working half.
- 7) Measure shear strength of the core samples of the working half using vane shear tester (see 3.4.4).
- 8) Take samples successively from the working half using 7-cc-plastic-cubes.

Finally all the core samples were packed into D-tubes, and then archive halves were transported to the Kochi Institute for Core Sample Research, JAMSTEC and working halves to the Laboratory of Global Paleoenvironment (Motoyama's Laboratory), University of Tsukuba.

The recovered three core samples are described in detail below.

[HFPC01 and HFPL01]

To measure the heat flow along the previous multi-channel survey line, HFPC01 was conducted on a flat surface in the Hokkaido rise at 38°59.64'N and 145°14.91'E. The water depth was 5404 m.

The piston and pilot cores are 274.5 cm and 83.5 cm long, respectively (Fig. 3.5-5). The pilot core penetrated probably twice into the seabed, because a surface oxidized layer can be seen at two horizons of 0-3 and 54-56 cm.

The core sediment is predominantly olive gray (7.5Y4/1) diatom silty clay, which is composed of mostly diatoms, siliciclastic grains, clay particles, and volcanic glasses. At 247-274.5 cm, the diatom silty clay is interbedded with dark greenish gray (10GY3/1) faint laminae in places. Olive black (7.5Y3/2) medium to fine volcanic ash layer having upward fining structure is seen at 105-107 cm-below-sea-floor (hereafter cm-bsf). Light gray (5Y7/1) fine volcanic ash layer is at 139-144 cm-bsf.

Shear strength increases progressively from about 0 to about 15 kPa with increasing depth, because of burial consolidation of the sediments.

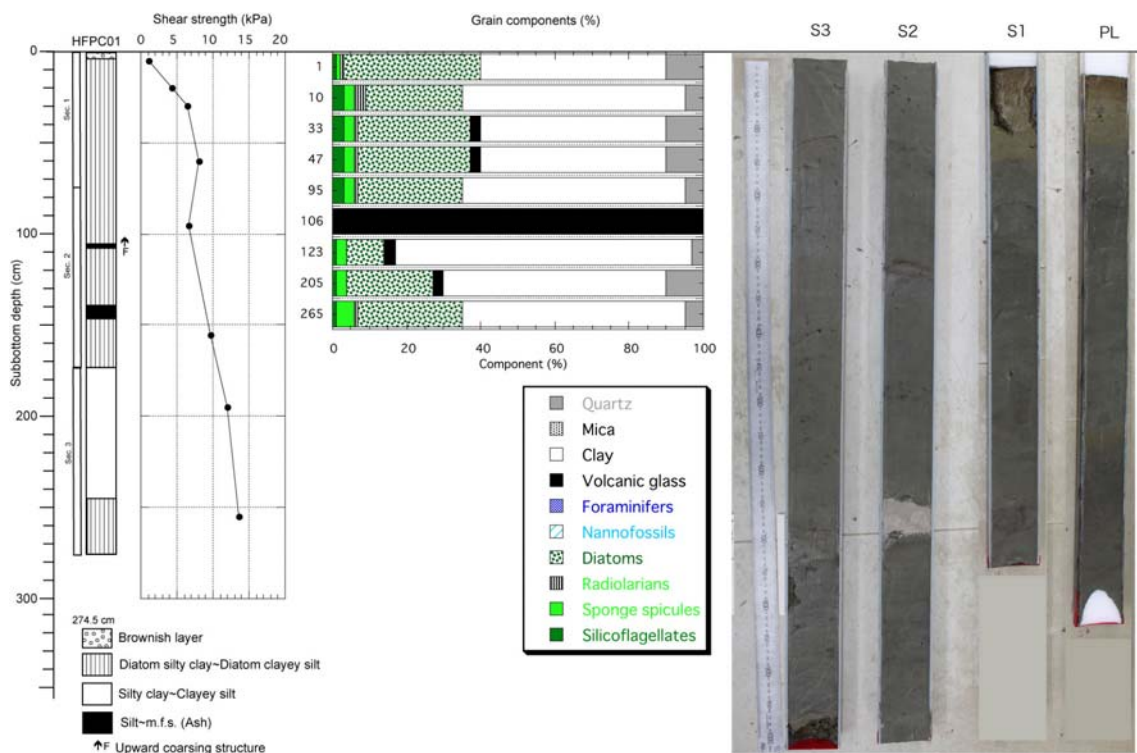


Figure 3.5-5. Summary of HFPC01.

[HFPC02 and HFPL02]

To measure the heat flow along the previous multi-channel survey line, HFPC02 was conducted on a seaward gentle slope at 38°04.90'N and 144°35.61'E. The water depth was

5749 m.

The piston and pilot cores were recovered 287.5 and 66 cm long, respectively (Fig. 3.5-6). The pilot core penetrated probably twice into the seabed, because a surface oxidized layer can be seen at two horizons of 0-4 and 50-54 cm. Therefore original length of the pilot core by the first penetration is probably 16 cm long, and that of the second penetration is about 50 cm long or more.

The piston core sediments are predominantly olive black (10Y3/2) diatom silty clay including many volcanic glasses as hemipelagic clayey sediments. Three black (7.5Y2/1 and 3/1) scoriaceous volcanic ash layers are seen at 80-81, 184.5-185.5 and 224.5-225.5 cm-bsf.

Shear strength increases successively about 15 kPa at ~200 cm-bsf with increasing depth, because of burial consolidation of the sediments. The strength could not be measured below ~200 cm-bsf, because of high consolidation degree.

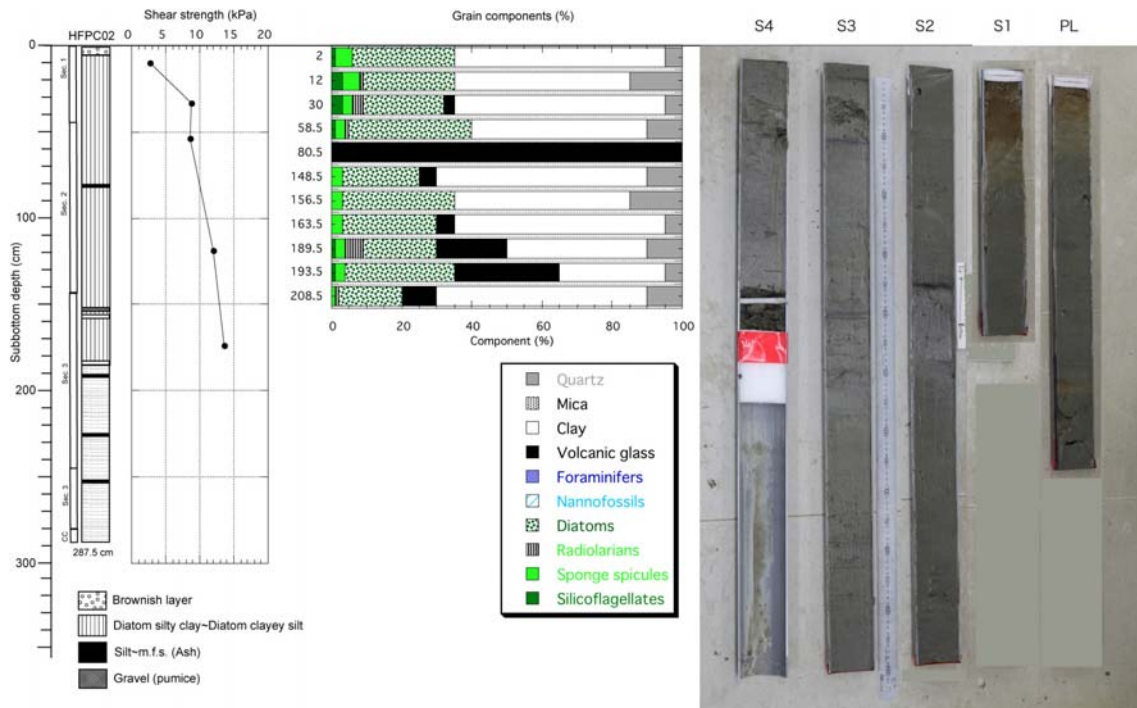


Figure 3.5-6. Summary of HFPC02.

[7K#462 C01]

To measure thermal and electric conductivities, this core was collected from the flat mud surface near the OBEM site A5 (40°15.16'N, 145°40.40'E) using a MBARI corer of unmanned-submersible Kaiko 7000II. The water depth was 5216 m.

This core is 27.5 cm long (Fig. 3.5-7). It is composed of mainly olive black (7.5Y3/2) diatom silty clay with a surface oxidized layer of dark olive brown (2.5Y3/3) diatom silty clay.

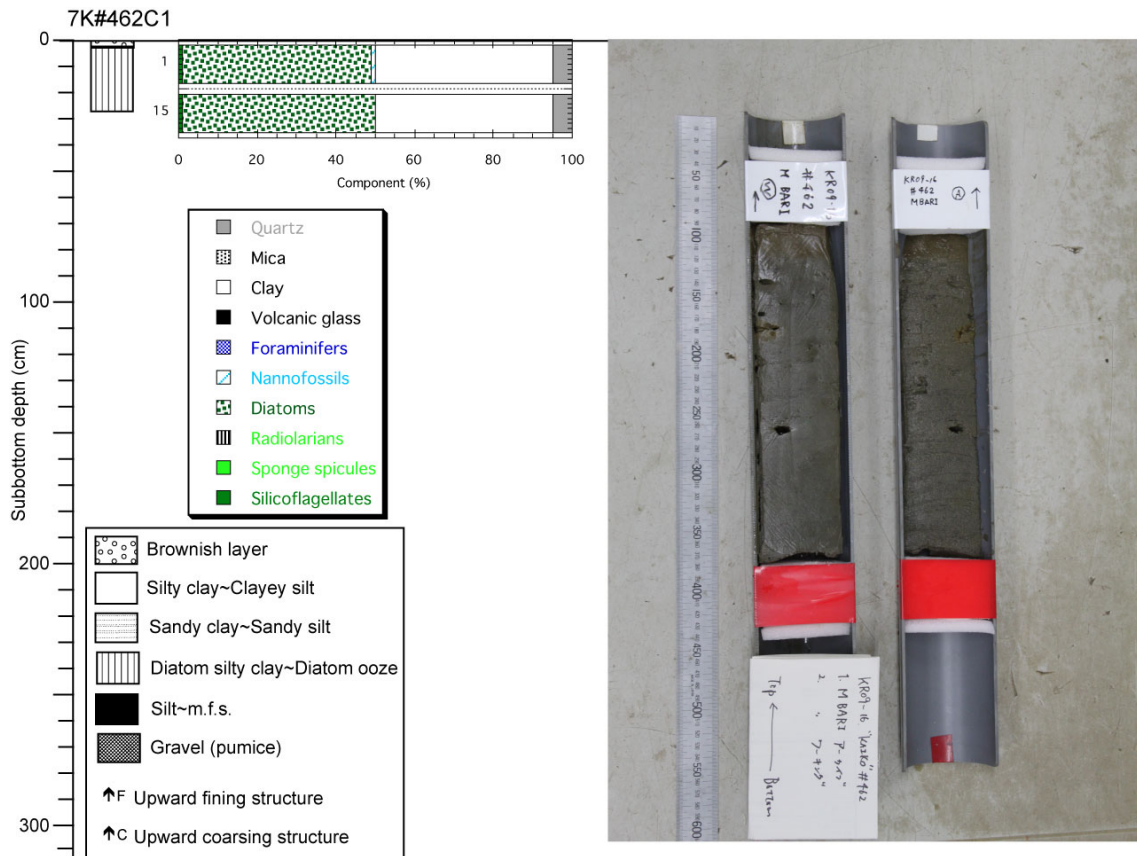


Figure 3.5-7. Summary of 7K#462 C01.

### 3.5.4. Recovery of LT-OBEMs

We successfully recovered five LT-OBEMs in this cruise. Two of them, TT4 at site A1 (previously called LEM01) and TT1 at site B1 (LEM02), were deployed during R/V Kairei KR08-10 cruise in September, 2008 and the other three, ERI12 at site B2 (LEM04), ERI1 at site C1 (LEM03), and ERI2 at site C4 (LEM05), were deployed during R/V Tansai-maru KT09-8 cruise in June, 2009. The site locations are plotted in Fig. 3.5-8 and listed in Table 3.5-3. For TT4 (type-1 OBEM), an acoustic transducer was hung from the portside deck manually. The hull bottom transducer and SSBL system were utilized for the other four OBEMs (type-2 OBEMs). After sending weight-release command, slant range between the ship and OBEM and ship's position were measured and ascent rate was calculated (Table 3.5-3). By tracking OBEM, its surface time was accurately predicted. And, OBEM was quickly found with the ship looking into the direction of radio beacon signal and tracked position (for type-2 OBEMs) after the surfacing. The OBEM was hooked from starboard deck and pulled around the stern, and then lifted on deck using the A-frame and a capstan.

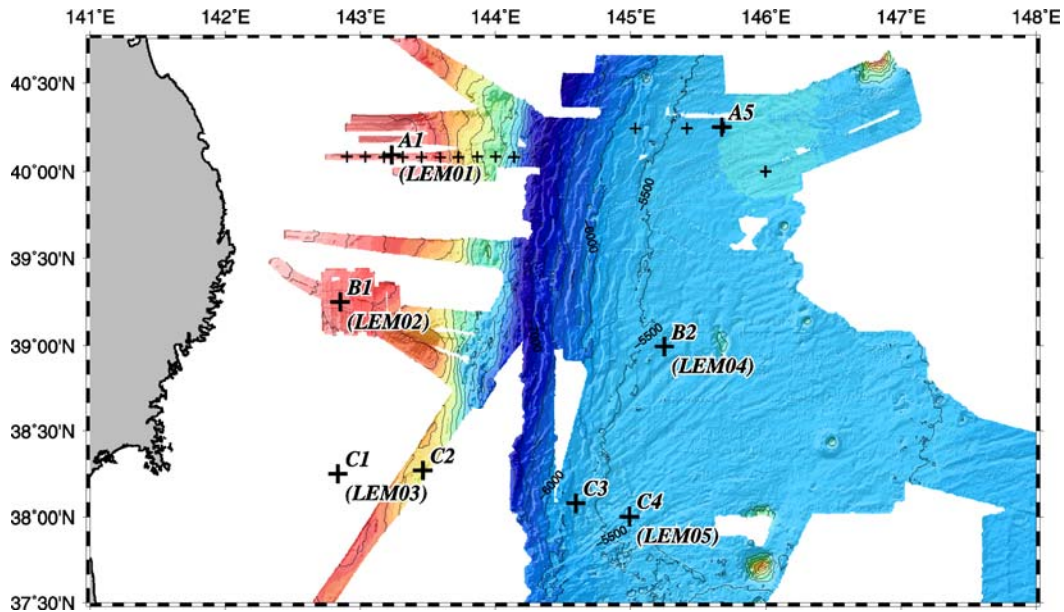


Figure 3.5-8. EM site locations superimposed on bathymetric map created based on multi-narrow beam sounding (SeaBeam) data. Big crosses with label indicate the sites that the OBEMs were recovered during this cruise and small crosses indicate the sites that the data were collected in the past experiments, respectively.

Table 3.5-3. Site locations and ascent rate of LT-OBEMs.

Site	OBEM	Latitude	Longitude	Depth	Ascent Rate
A1 (LEM01)	TT4	40° 05.733' N	143° 13.897' E	1230 m	40.0 m/min.
B1 (LEM02)	TT1	39° 14.832' N	142° 51.069' E	1686 m	30.0 m/min.
B2 (LEM04)	ERI12	38° 59.589' N	145° 14.923' E	5383 m	32.2 m/min.
C1 (LEM03)	ERI1	38° 14.986' N	142° 49.959' E	1429 m	33.2 m/min.
C4 (LEM05)	ERI2	38° 00.180' N	144° 59.445' E	5414 m	31.8 m/min.

All OBEMs recorded data for full time of the observation periods. The clock of each OBEM was compared with reference (GPS) clock immediately after the recovery. The time difference between them for each OBEM is listed in Table 3.5-4 and the time stamp of the record will be corrected in analysis assuming linear shift during the observation. The data were downloaded to laptop PC through serial (for TT1 and TT4) or USB (for ERI1, ERI2, and ERI12) communication. The raw time series data is plotted in Figures 3.5-9 - 3.5-13. The quality is very good except for the electric field of TT1 at site B1 (LEM02).

Table 3.5-4. Clock information of LT-OBEMs.

Site	Set time (TZ: +0h)	Compared time (TZ: +0h)	Time difference (OBEM-Ref.)	Sampling rate
A1 (LEM01)	2008-09-05T00:51:00	2009-11-01T21:53:55	19.0 sec.	60 sec.
B1 (LEM02)	2008-09-07T09:38:01	2009-10-31T22:56:46	46.0 sec.	60 sec.
B2 (LEM04)	2009-06-01T07:56:14	2009-11-03T22:17:36	10.3 sec.	60 sec.
C1 (LEM03)	2009-06-04T08:45:41	2009-10-30T23:31:36	14.9 sec.	60 sec.
C4 (LEM05)	2009-06-03T05:10:38	2009-10-31T09:22:10	17.5 sec.	60 sec.

## Site LEM01 (TT4) raw data

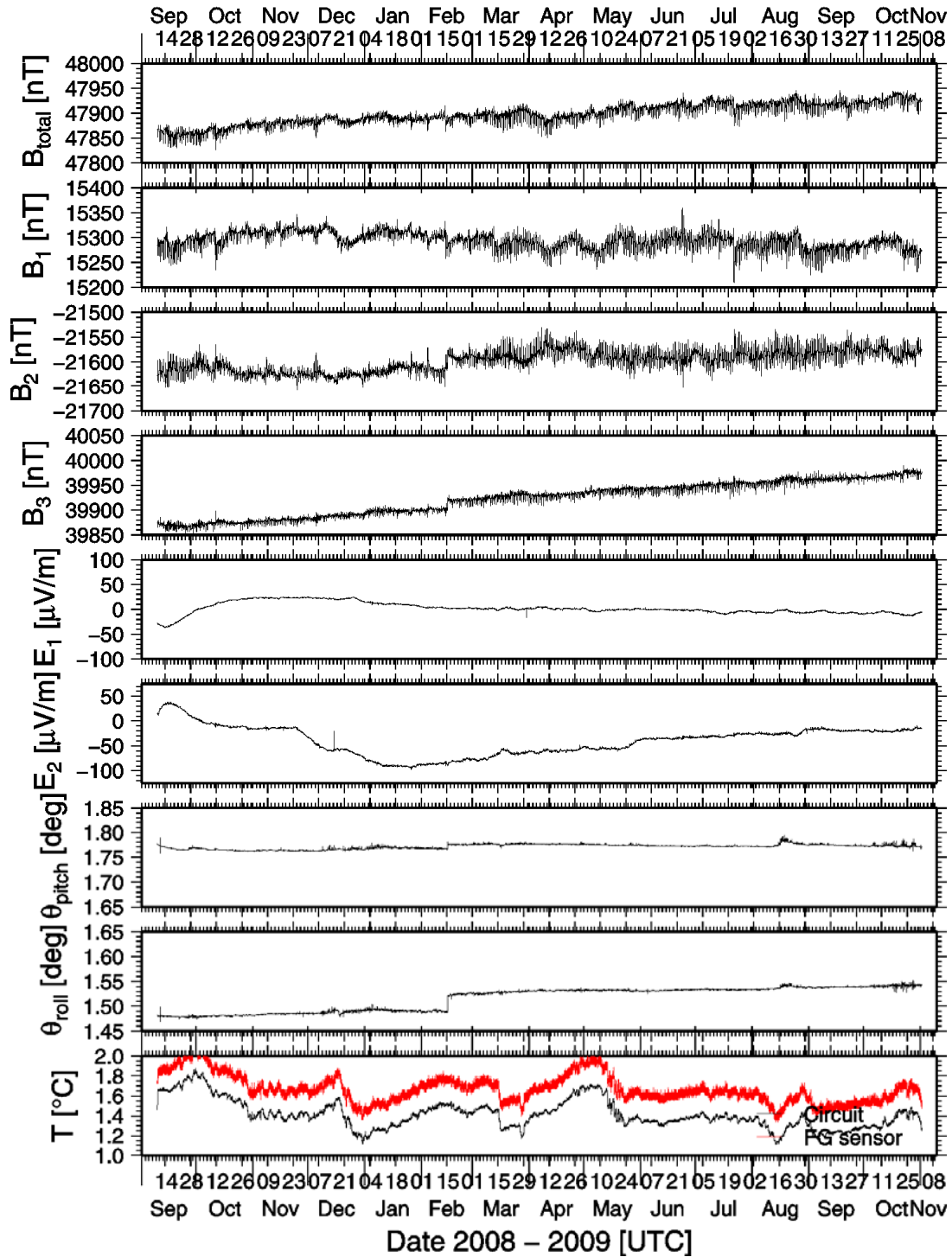


Figure 3.5-9. Raw time series obtained by LT-OBEM TT4 at site LEM01. From the top to the bottom, total magnetic intensity calculated from the three components, three components of the magnetic field, two components of the electrical field, two components of the instrumental tilt, and temperatures on the flux gate sensor and circuit, respectively.

# Site LEM02 (TT1) raw data

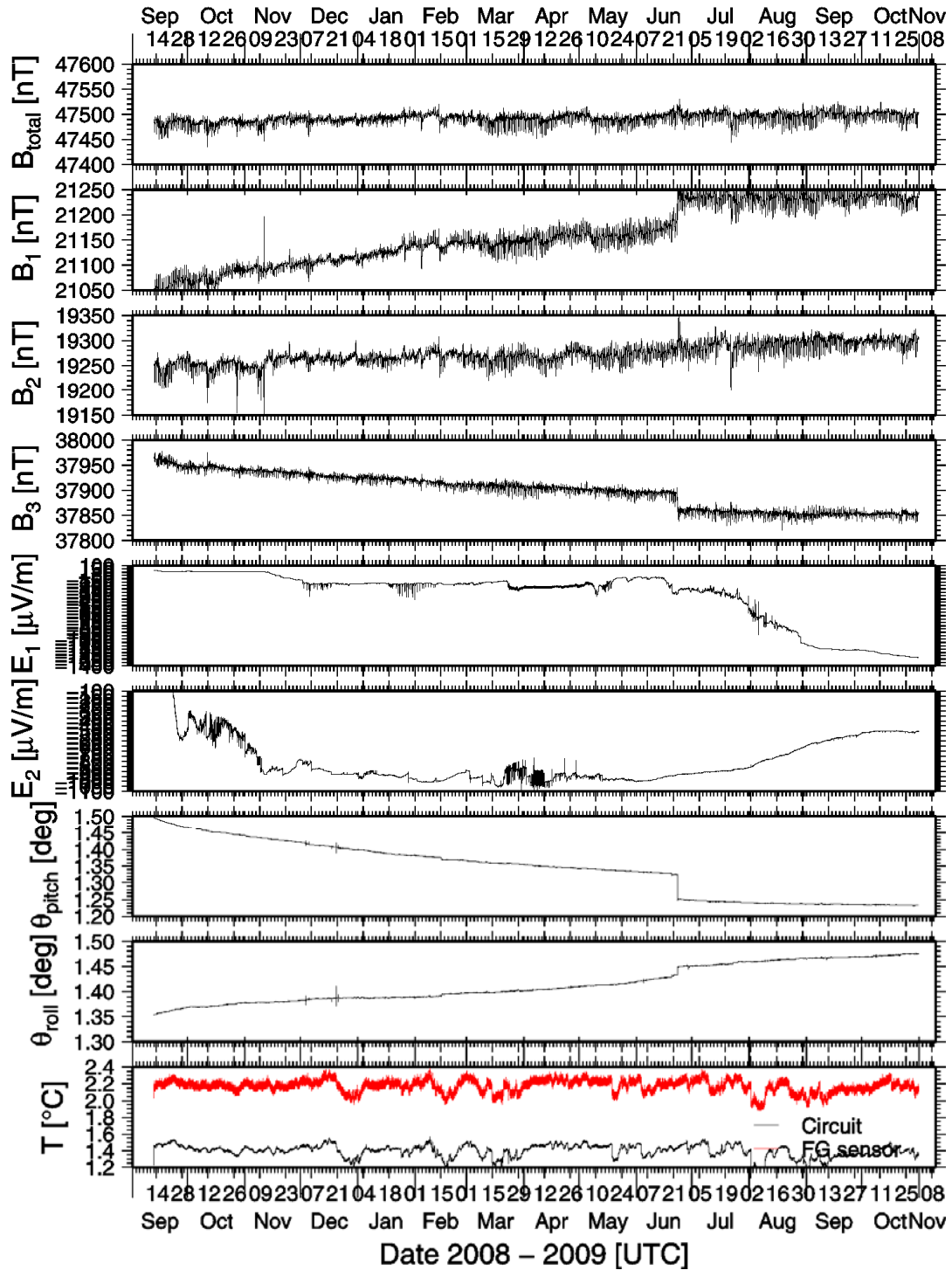


Figure 3.5-10. Raw time series obtained by LT-OBEM TT1 at site LEM02. The plotted components are the same as Figure 3.5-9.

## Site LEM03 (ERI1) raw data

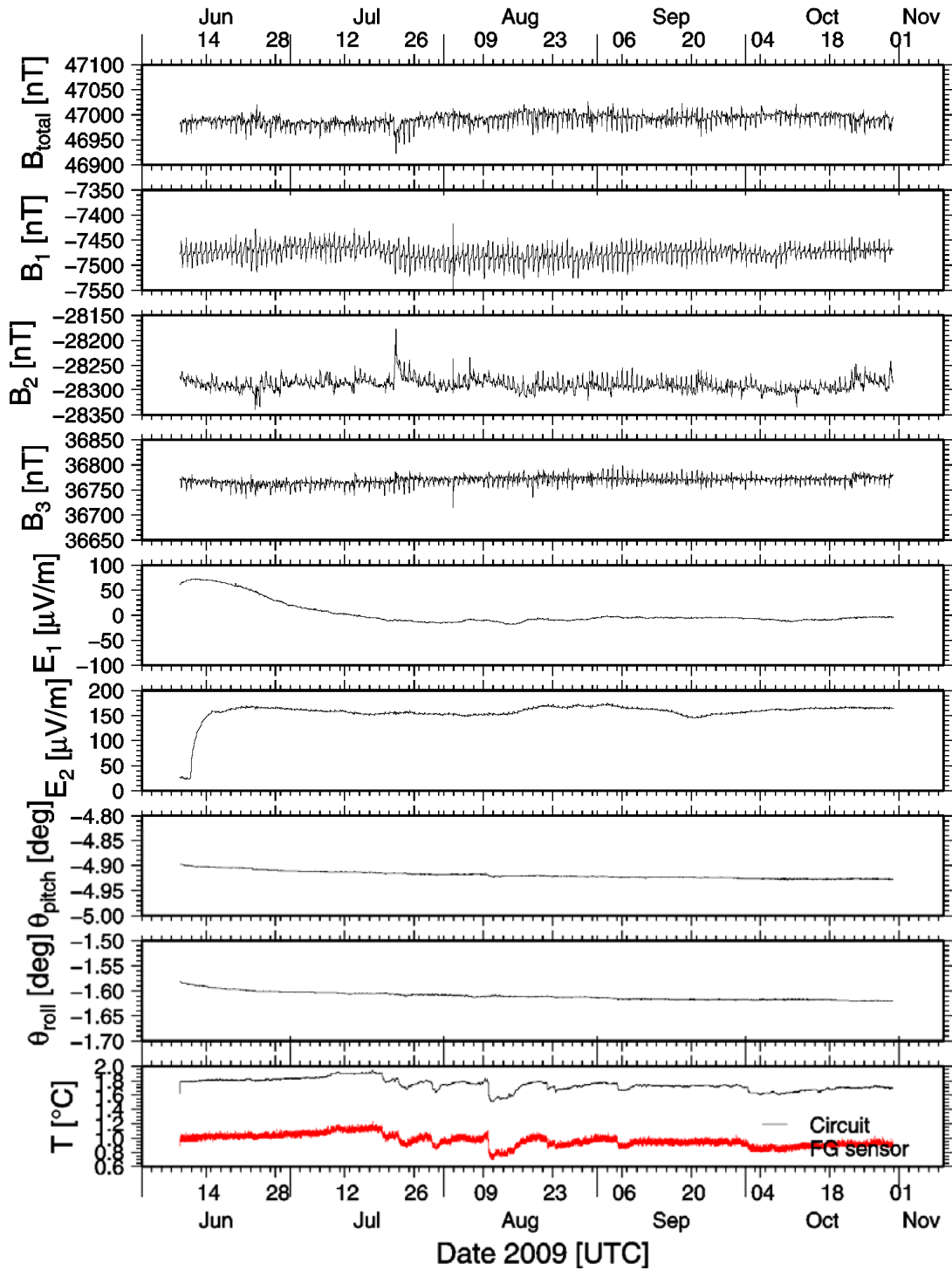


Figure 3.5-11. Raw time series obtained by LT-OBEM ERI1 at site LEM03. The plotted components are the same as Figure 3.5-9.

# Site LEM04 (ERI12) raw data

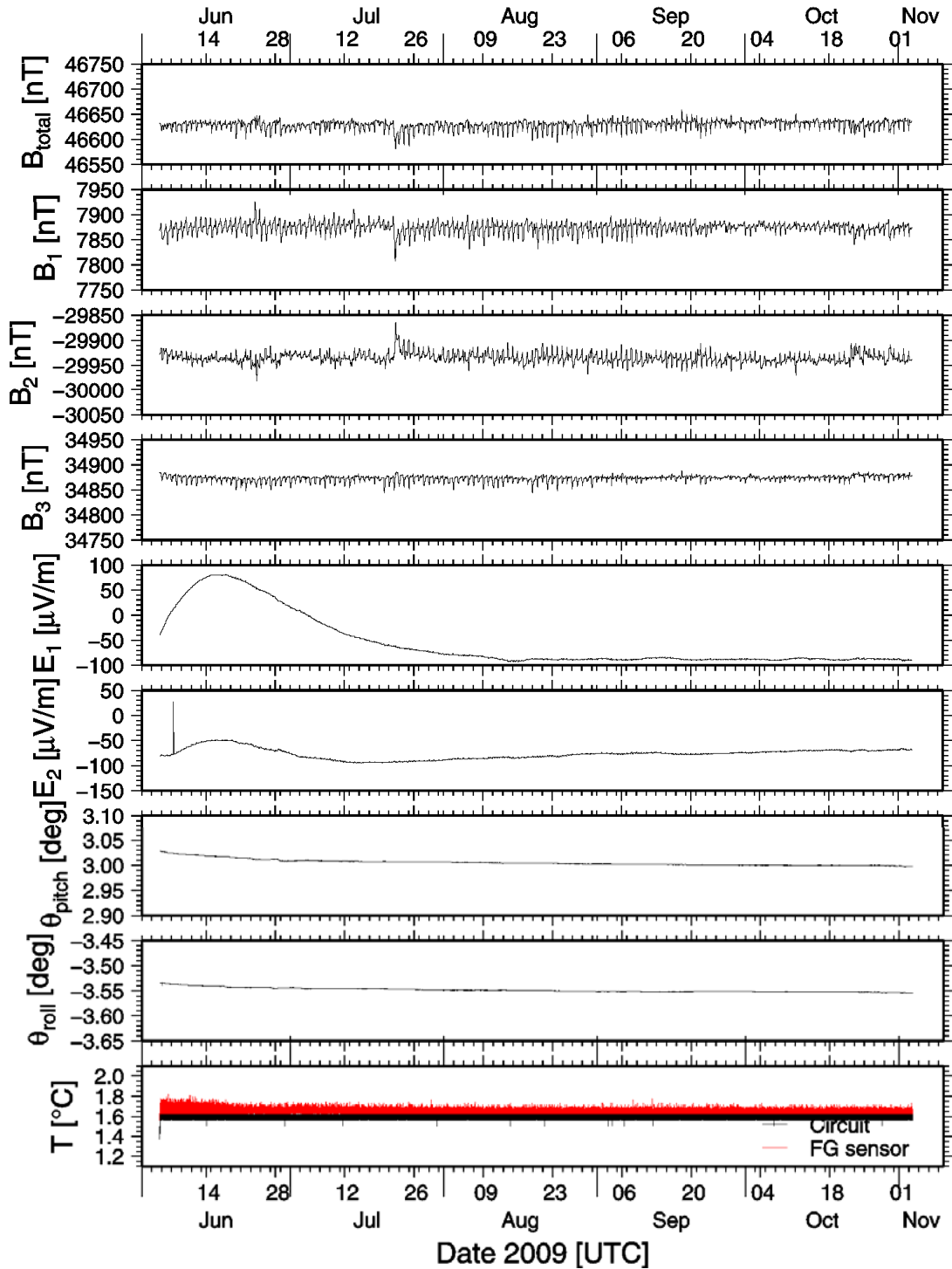


Figure 3.5-12. Raw time series obtained by LT-OBEM ERI12 at site LEM04. The plotted components are the same as Figure 3.5-9.

# Site LEM05 (ERI2) raw data

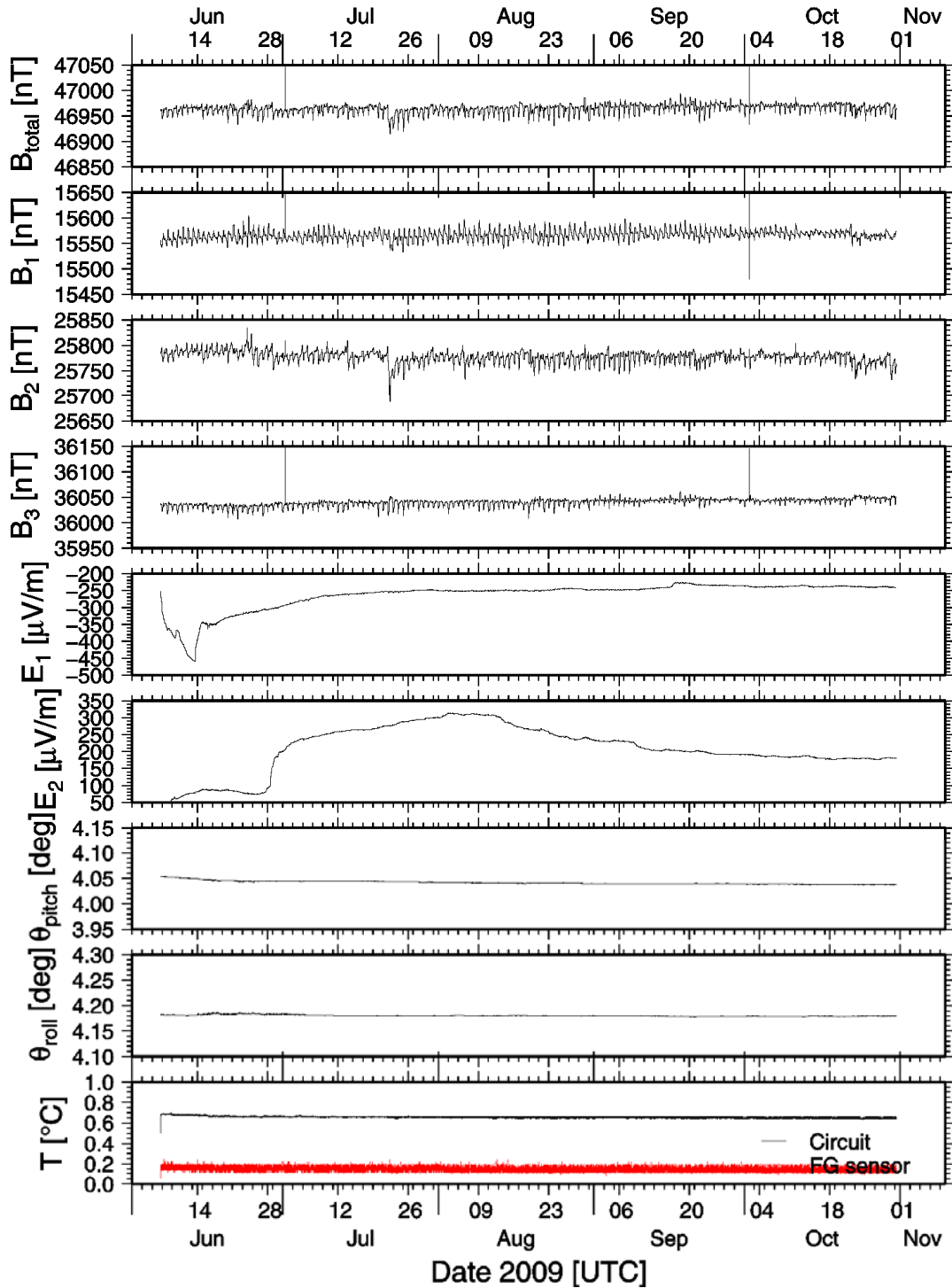


Figure 3.5-13. Raw time series obtained by LT-OBEM ERI2 at site LEM05. The plotted components are the same as Figure 3.5-9.

### 3.5.5. HF-OBEM operation

We successfully deployed and recovered three HF-OBEMs in this cruise (Site C2, Site C3, and Site A5 in Fig. 3.5-8). Table 3.5-5 shows the specification of each OBEM. We could track the HF-OBEM's positions by SSBL system of R/V Kaiei because the communication frequency of our acoustic system matched ship's SSBL system. Landing position of each OBEM was settled by SSBL system (Table 3.5-6). Figure 3.5-14 portrayed the detailed map with the launched and settled position of each OBEM.

They started ascending within about 15 minutes after sending the acoustic release signal. We also could track the OBEM position while they were ascending. The small batteries (10 days battery life) were used in this cruise. Therefore, the estimated ascending rate, which is 50 (m/min.) and over (Table 3.5-7), was faster than the average reported by Kasaya and Goto (2009). We could find the surfaced OBEM easily because the precise surface time by SSBL system.

All recovered OBEMs recorded data with 8Hz sampling rate. After finishing recovery operation, the time difference between the OBEM's clock and the laptop pc synchronized by NTP server unit was measured. Their results and other clock information were shown in Table 3.5-7. Obtained EM data were very clean. Figures 3.5-15 and 3.5-16 present the raw time series obtained by HF-OBEM at C2 and C3. Total magnetic variation in each figure was calculated by the three components fluxgate magnetometer.

Table 3.5-5. Specification of each HF-OBEM.

SiteID	OBEM ID	T.P. no.	Code	Flasher	R.Beacon	Dipole length
C2	JM102	JX-1176	4D-1	S12-019	S19-033 (JS1368)	4.44 (m)
C3	JM103	JX-1186	2A-1	S12-018	S12-030 (JS1365)	4.44 (m)
A5	JM100	JX-1173	4C-1	S12-013	S12-032 (JS1367)	4.44 (m)

Table 3.5-6. Site locations of HF-OBEMs.

SiteID	Lat(seafloor)	Lon(seafloor)	Depth(m)	Lat(deploy)	Lon(deploy)	Start time(JST)
C2	38-16.2024	143-27.7686	3241	38-15.8107	143-27.4678	2009/10/31 9:30
C3	38-4.8078	144-35.7404	5741	38-4.2582	144-35.9980	2009/10/31 14:30
A5	40-15.1591	145-40.4049	5216	40-15.0331	145-40.4570	2009/11/6 10:00

Table 3.5-7. Recovery and clock information of HF-OBEM.

SiteID	Recovery data(JST)	Ascent rate	Clock set time (JST)	Clock compare time (JST)	Time difference (sec)
C2	2009/11/9	53 m/min	2009/10/31 8:22:38	2009/11/9 8:37:30	+1.964 sec
C3	2009/11/8	51 m/min	2009/10/31 10:33:17	2009/11/8 17:33:36	+0.446 sec
A5	2009/11/7	53 m/min	2009/11/6 7:48:35	2009/11/7 16:31:55	+0.205 sec

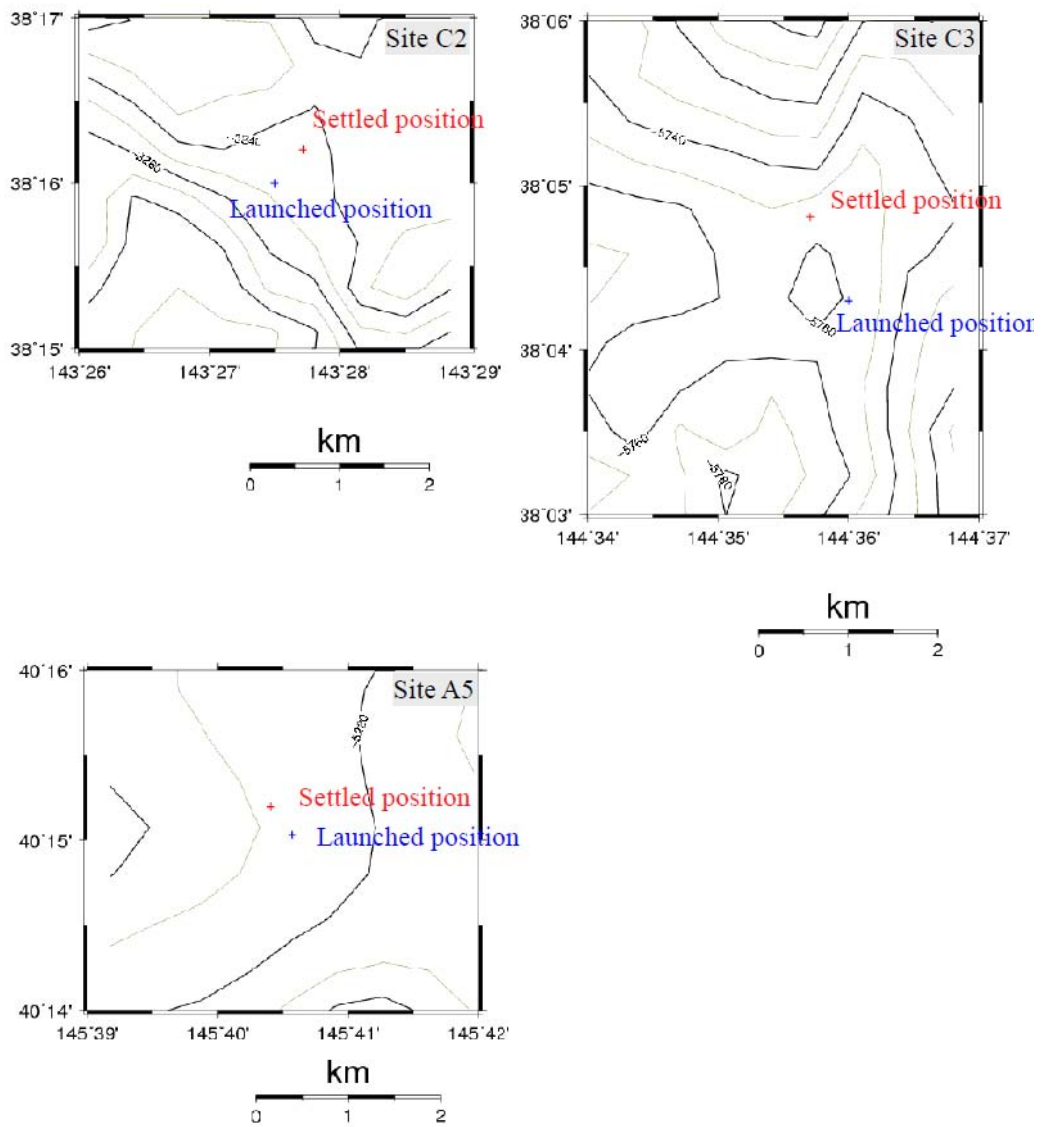


Figure 3.5-14. Detailed map around the HF-OBEM sites. Red and blue cross shows the settled and launched position, respectively.

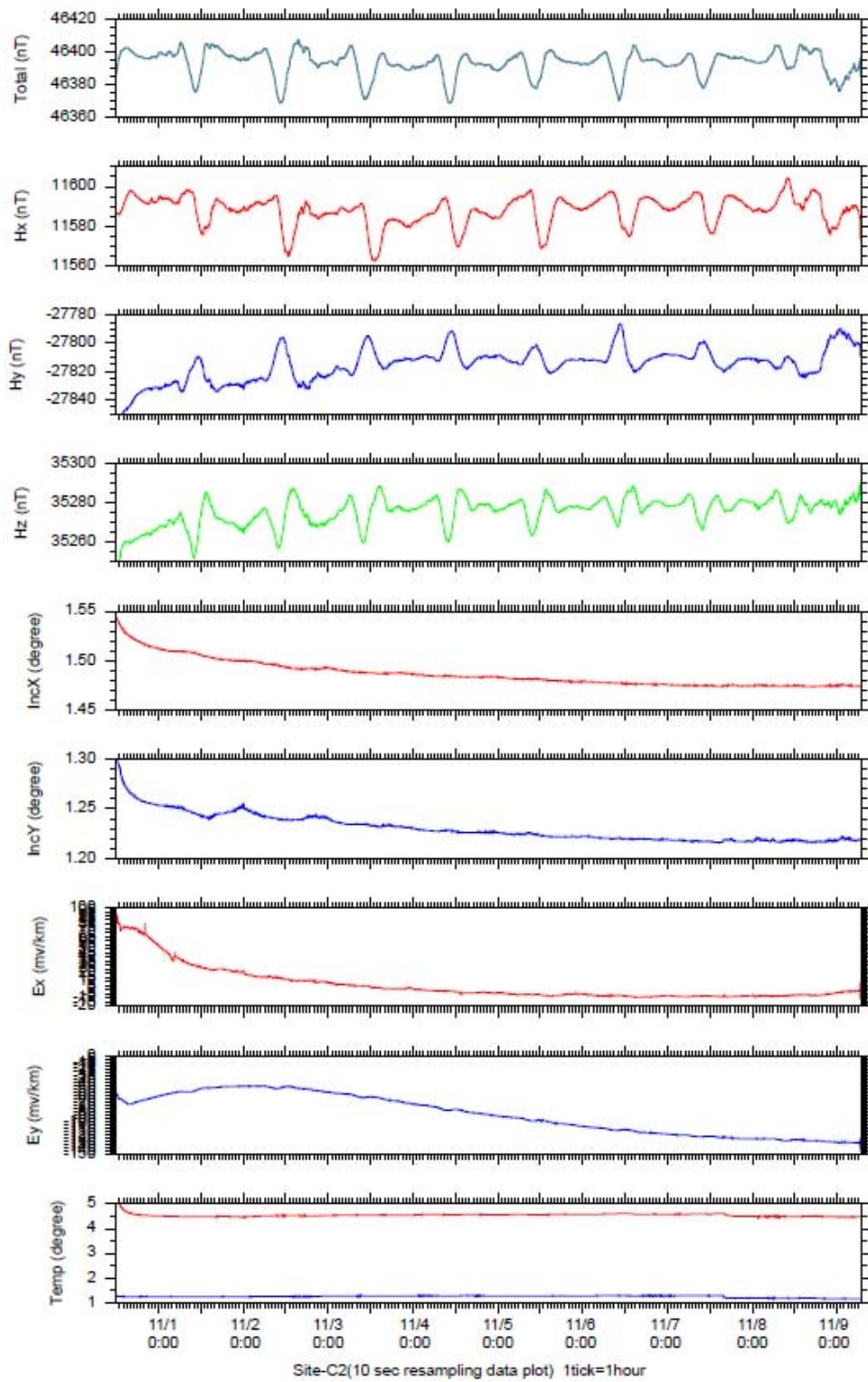


Figure 3.5-15. Raw time series at site C2 obtained by HF-OBEM (JM102). The total magnetic intensity time series at the top graph was calculated from the three components fluxgate magnetometer.

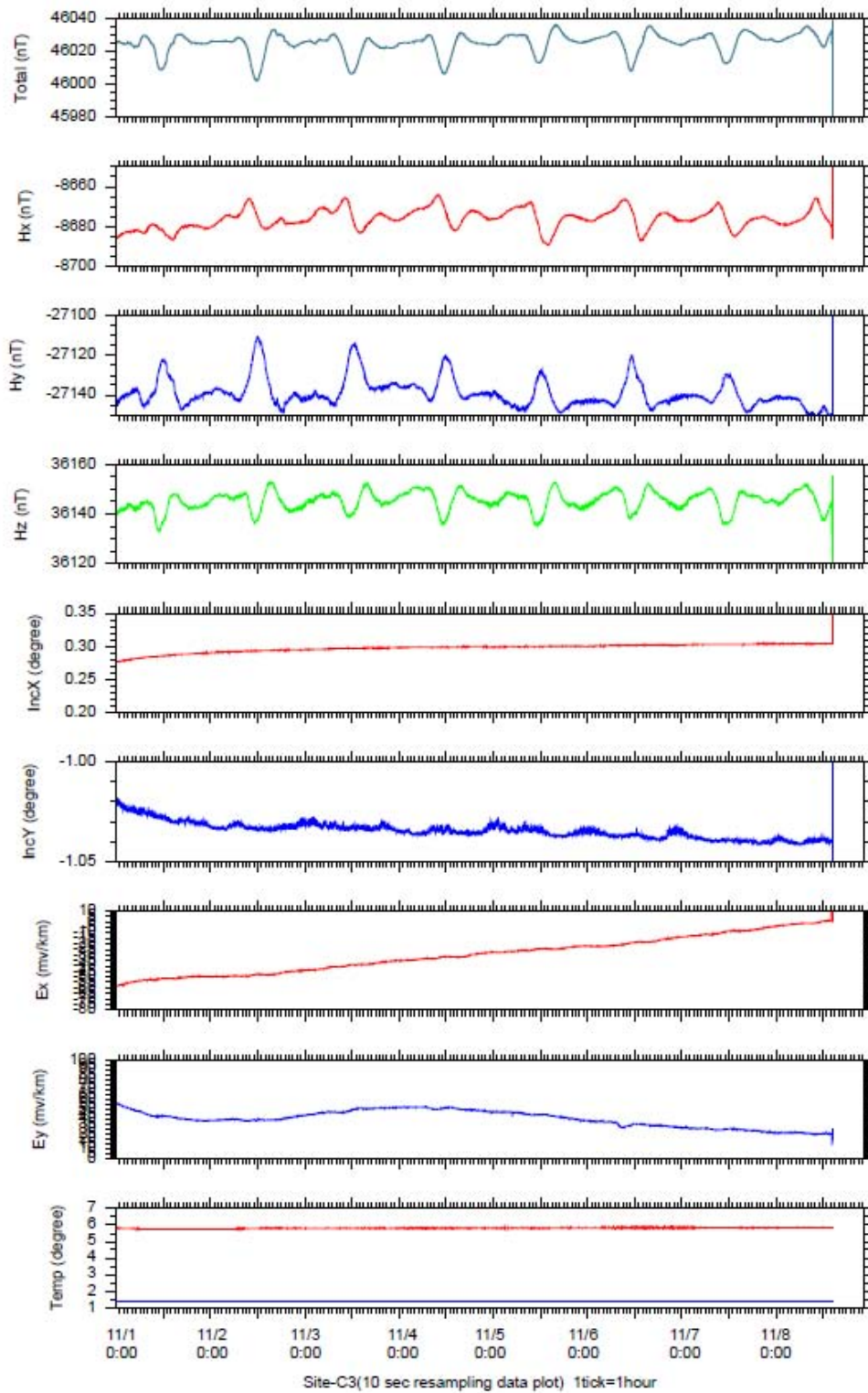


Figure 3.5-16. Raw time series at site C3 obtained by HF-OBEM (JM102). The total magnetic intensity time series at the top graph was calculated from the three components fluxgate magnetometer.

### 3.5.6. Kaiko CSEM experiment

The ROV “Kaiko 7000II” dived to the OBEMs (sites A5 and C3). These two sites with water depth of 5200 - 5700m were selected because of their contrastive characters: the site A5 is located near a high heat-flow anomaly, and another one is located further south with normal heat-flow values as a reference. As described in 3.4.6, we used a new controlled-source electromagnetic (CSEM) system operated by the ROV "Kaiko 7000II". A 20m-length cable and a transmitter unit were attached to the vehicle of ROV. During Dive #461 - #463 of Kaiko 7000II, the transmitter on the Kaiko vehicle sends the artificially controlled electric current (with squared waves) on the seafloor using the 20m-dipole cable extended horizontally. An OBEM (ocean bottom electromagnetometer) receive the EM signal (Fig. 3.5-17). The details of each dive are summarized as follows.



Figure 3.5-17. Left: ROV Kaiko recovered from the CSEM experiment. The 20m-dipole cable can be seen, extended from sample basket. Right: OBEM taken by ROV Kaiko Camera at site A5.

[Dive 461]

The Kaiko 7000II dived at site A5. Artificial electric current was sent at seafloor southern from an OBEM landing on the seafloor. The source-receiver distance was 130 – 280 m. However, the transmitter had electrical leakage at the pressure case of TX-unit (Fig. 3.5-18). Also, received potential data by the RX unit attached to the Kaiko 7000II was unstable. Due to these troubles, a little data was obtained.



Figure 3.5-18. Electrical corrosion by leakages at the TX unit.

[Dive 462]

The Kaiko 7000II dived at site A5 again. Artificial electric current was sent at seafloor western from the OBEM landing on the seafloor. The source-receiver distance was 58 – 200 m. For this dive, we attached an additional recorder (so called “SP recorder”) and electrodes to the ROV for measuring the electric field around the ROV (see Fig. 3.4-16). It was an alternate for the original RX unit which was not stable at the dive 461. Both OBEM and SP recorder received the artificial electric signal successfully. Because the leakage trouble at the TX unit was discovered again, the data analysis should include a correction for the leakage current from the TX unit.

[Dive 463]

The Kaiko 7000II dived at site C3. No leakage trouble was found. Due to the strong water current near the seafloor, it was fairly difficult to move the vehicle and launcher of the Kaiko 7000II as we want. As a result, the only one shooting at seafloor was achieved at 420 m NNW from an OBEM landing on the seafloor. Although the transmitter still had a trouble and the current amplitude is quite limited ( $< 5A$ ), both OBEM and SP recorder received the artificial electric signal successfully.

As a result, the electric signal sent from the ROV Kaiko 7000II was successfully received by the OBEM on the seafloor with source-receiver separation of 58 – 420 m. Figure 3.5-19 shows the electrical potential recorded by OBEM at the dive 462. At the shorter source-receiver separations (58 – 250 m), we can easily recognize the squared waves in the raw time series. Further separation requires the data stacking to improve the S/N ratio. Figure 3.5-20 is an example demonstrating the effect of stacking. At the far site with source-receiver separation of 420 m, a square wave in raw time series is not clearly recognized. But after stacking, we can easily find the sharp drop of potential value. On the basis of the potential drop synchronized to the artificial signal, we can estimate the apparent resistivity at the seafloor.

Since the seawater conductivity is measurable with the CTD sensor attached to the Kaiko vehicle, we can obtain the electrical conductivity distribution below the seafloor.

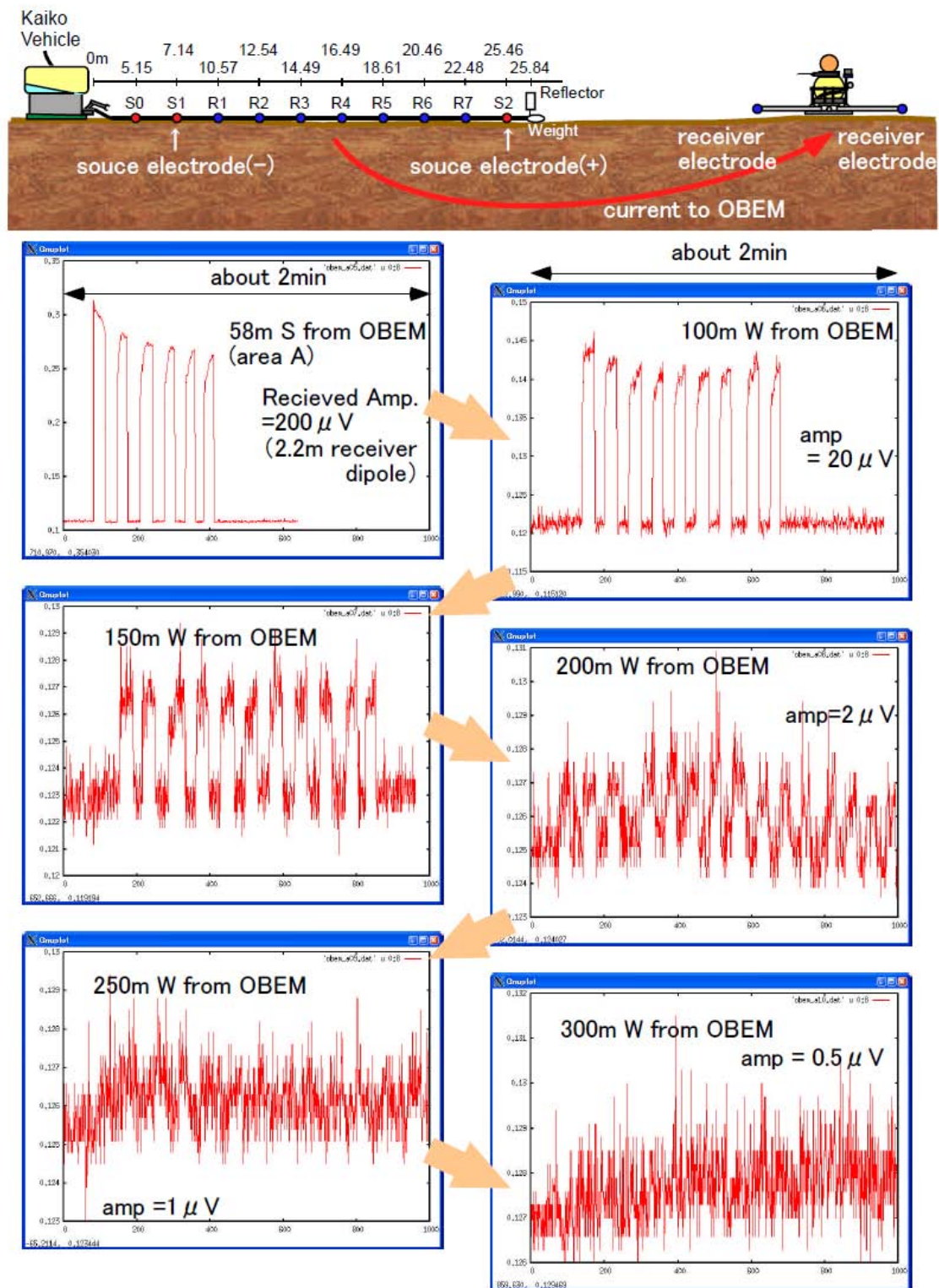


Figure 3.5-19. Electrical potential recorded by OBEM at Dive 462 (raw time series without any filtering). The dipole length of the receiver was 2.2 m.

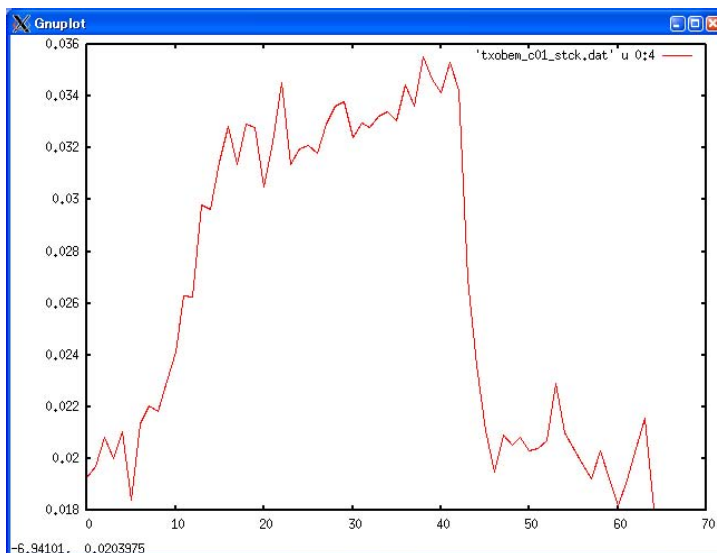
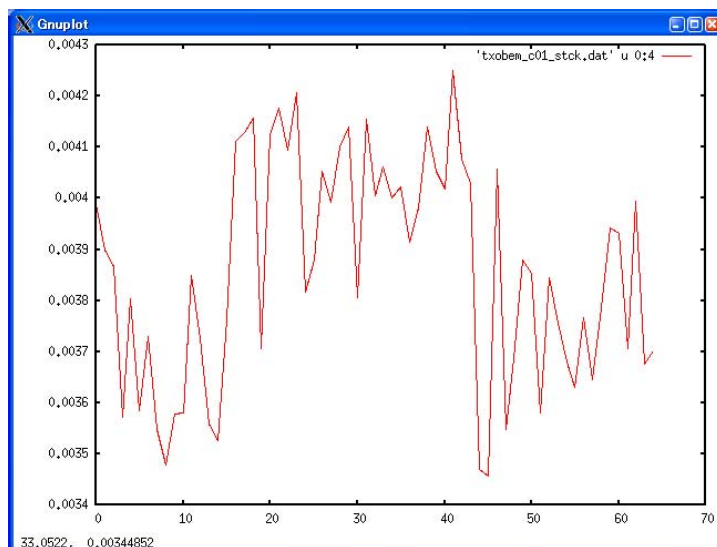


Figure 3.5-20. Recorded electric signal by the OBEM at site C3 (Dive 463). The source-receiver separation is about 420 m. Time series during 4 seconds are shown. Upper: raw time series. Lower: 65 waves are stacked to create one signal.

We also check our system in the middle of seawater. We can obtain the seawater conductivity by our system. The value is also estimated by the CTD sensor, and we can compare these two and calibrate our system. Figure 3.5-21 is a raw data at the calibration in the seawater. The estimated seawater conductivity is almost same as one by CTD. Therefore, we believe that artificial electric current from our system is not severely distorted by the ROV frame and the main cable for ROV.

This experiment, the ROV-CSEM survey, is the first trial and success in the world. The maximum source-receiver distance was 420 m, which is greatly advanced from the previous experiment in the KR08-10. This successful result implies us that the ROV-CSEM survey is technically achieved. The data analysis is now undergoing and will allow us the discussion

about near-seafloor resistivity structure of the Pacific plate.

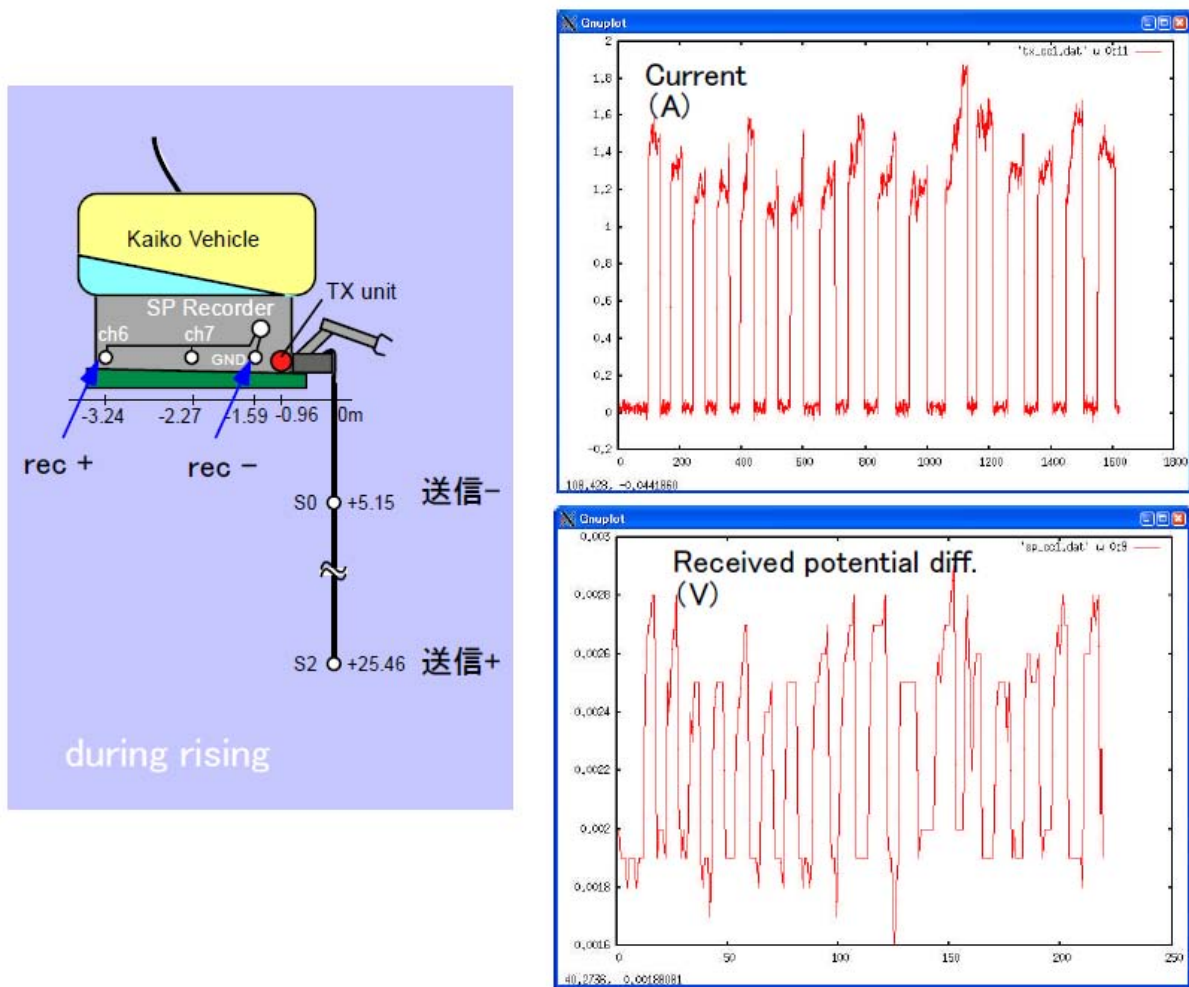


Figure 3.5-21. Time series data at the calibration of our system. The waveform of sending current and received potential is very similar.

We also deployed three HF-OBEM (High-frequency OBEM) at three sites on the Pacific plate. Two of them were used for the ROV-CSEM experiment described above. All of them were successfully recovered from the seafloor. Data recovery rate is also fine. One of the great news for us is successful of 24 bit A/D converter for recording electric field. Such new A/D converter gives us highly resolved electric field on the seafloor. In Figure 3.5-20, we can find the squared wave form, although it is not clear. In the left-bottom graph in Figure 3.5-19 (300m W from OBEM), the squared wave form is hard to be seen. The former is recorded by a modified OBEM with 24 bit A/D, and the latter is by the conventional one. As a result, we confirmed the stableness and effectiveness of our new 24 bit A/D converter for marine CSEM experiment.

The data obtained by OBEM will be analyzed with two different techniques: the Magnetotelluric (MT) sounding and the controlled-source electromagnetic (CSEM) sounding. Former will give us information of the uppermost mantle and crust. The latter is useful for estimation of shallow crustal information. These results will be helpful for discussion about the cause of anomalous high heat flow on the Pacific plate.

### **3.5.7. Bathymetry and geophysical survey**

Bathymetry and geophysical mapping surveys were made mainly at night in the vicinity of the 40°15'N line and around 39°N. The surveyed lines are listed in the Appendices (7.2). On all the lines, measurements of gravity and three components of the geomagnetic field were conducted with instruments on board as well as bathymetry mapping with a SeaBeam system. The total intensity of the geomagnetic field was measured with a proton precession magnetometer along some selected ENE-WSW lines on the seaward side of the Japan Trench (cf. 7.2). We also made 3.5 kHz subbottom profiling (SBP survey in 7.1) around piston coring sites for imaging structures in surface sediments.

## **4. Notice on Using**

This cruise report is a preliminary documentation as of the end of the cruise. It may not be corrected even if changes on content (i.e. taxonomic classifications) are found after publication. It may also be changed without notice. Data on the cruise report may be raw or not processed. Please ask the Chief Scientist for the latest information before using.

Users of data or results of this cruise are requested to submit their results to Data Integration and Analysis Group (DIAG), JAMSTEC.

## **5. Acknowledgements**

We are grateful to Captain H. Tanaka, the officers and the crew of the R/V Kairei, ROV Operation Manager K. Hirata, and the operation team of the ROV Kaiko 7000II for skillful operations of the ship, ROV, and research equipment. We also extend our thanks to S. Hosoya, E. Hatakeyama, Y. Matsuura, A. So, and Y. Fuwa for giving us great assistance in research works throughout the cruise. The staff of the Operation Group, Research Vessel Operation Department, Marine Technology Center, especially T. Hirai, made excellent arrangements for the cruise.

The research conducted on this cruise was partly supported by Japan Society for the Promotion of Science through a Grant-in Aid for Scientific Research (19340125).

## 6. References

- Fujie, G., J. Kasahara, R. Hino, T. Sato, M. Shinohara, and K. Suyehiro, A significant relation between seismic activities and reflection intensities in the Japan Trench region, *Geophys. Res. Lett.*, 29, 7, 10.1029/20, 2002.
- Goto, T., H. Mikada, K. Suyehiro, K. Yamane, L. Lewis, A. Orange, E. Nichols, and S. Constable, Electrical conductivity structures across seismically active and less active zones on the subducting Pacific plate, off northeast Japan, *Eos Trans. AGU*, 82(47), Fall Meet. Suppl.: Abstract GP21A-0249, 2001.
- Hamamoto, H., M. Yamano, and S. Goto, S., Heat flow measurement in shallow seas through long-term temperature monitoring, *Geophys. Res. Lett.*, 32, L21311, doi:10.1029/2005GL024138, 2005.
- Hirano N, K. Kawamura, M. Hattori, K. Saito, and Y. Ogawa, A new type of intra-plate volcanism; young alkali-basalts discovered from the subducting Pacific Plate, northern Japan Trench, *Geophys. Res. Lett.*, 28, 2719-2722, 2001.
- Hirano N, E. Takahashi, J. Yamamoto, N. Abe, S.P. Ingle, I. Kaneoka, T. Hirata, J. Kimura, T. Ishii, Y. Ogawa, S. Machida, and K. Suyehiro, Volcanism in response to plate flexure, *Science*, 313, 1426-1428, 2006.
- Ito, A., G. Fujie, T. Tsuru, S. Kodaira, A. Nakanishi, and Y. Kaneda, Fault plane geometry in the source region of the 1994 Sanriku-oki earthquake, *Earth Planet. Sci. Lett.*, 223, 163-175, 2004
- Kasaya, T., and T. Goto, A small OBEM and OBE system with an arm folding mechanism, *Exploration Geophysics*, 40, 41-48, 2009.
- Kasaya, T., T. Goto, and R. Takagi, Marine electromagnetic observation technique and its development –For crustal structure survey–, *BUTSURI-TANSA*, 59, 585-594 (in Japanese with English abstract), 2006.
- Miura, S., N. Takahashi, A. Nakanishi, T. Tsuru, S. Kodaira and Y. Kaneda, Structural characteristics off Miyagi forearc region, the Japan Trench seismogenic zone, deduced from a wide-angle reflection and refraction study, *Tectonophysics*, 407, 165-188, 2005.
- Nakajima, J., and A. Hasegawa, Anomalous low-velocity zone and linear alignment of seismicity along it in the subducted Pacific slab beneath Kanto, Japan: Reactivation of subducted fracture zone?, *Geophys. Res. Lett.*, 33, doi:10.1029/2006GL026773, 2006.
- Oleskevich, D.A., R.D. Hyndman, and K. Wang., The updip and downdip limits to great subduction earthquakes: thermal and structural models of Cascadia, south Alaska, SW Japan, and Chile, *J. Geophys. Res.*, 104, 14965-14991, 1999.
- Sass, J.H., C. Stone, and R.J. Munroe, Thermal conductivity determinations on solid rocks - a comparison between a steady-state divided-bar apparatus and a commercial transient

- line-source device, *Jour. Volcanol. Geotherm. Res.*, 20, 145-153, 1984.
- Tsuru, T, J.-O. Park, N. Takahashi, S. Kodaira, Y. Kido, Y. Kaneda, and Y. Kono, Tectonic features of the Japan Trench convergent margin off Sanriku, northeastern Japan, revealed by multichannel seismic reflection data, *J. Geophys. Res.*, 105, 16,403-16,413, 2000.
- Von Herzen, R., and A.E. Maxwell, The measurement of thermal conductivity of deep-sea sediments by a needle-probe method, *J. Geophys. Res.*, 64, 1557-1563, 1959.
- Yamano, M., M. Kinoshita, and S. Goto, High heat flow anomalies on an old oceanic plate observed seaward of the Japan Trench, *Int. J. Earth. Sci*, 97, 345-352, 2008.
- Yamano, M., H. Hamamoto. K. Kawamura, S. Goto, Y. Kawada, and Y. Masaki, On the extent of the high heat flow anomaly observed seaward of the Japan Trench, Japan Geoscience Union Meeting 2009, J173-005 (abstract), 2009.
- Yamanaka, Y., and M. Kikuchi, Asperity map along the subduction zone in northeastern Japan inferred from regional seismic data, *J. Geophys. Res.*, 109, B07307, doi:10.1029/2003JB002683, 2004.

## 7. Appendices

### 7-1. Cruise Log

KR09-16 Shipboard Log:

Date Time Log

2009/10/30

Weather: fine but cloudy/ Wind direction: NNE Wind force: 3/ Wave: 3 m/ Swell: 3 m/ Visibility: 7 nautical miles (12:00 JST)

08:00 Onboard

09:00 Departure from JAMSTEC

10:00-10:45 Briefing about ship's life and safety

10:45-11:20 Scientific meeting

16:40-17:00 Pray for safety of cruise to KONPIRASAN

Transit to survey area" F"

2009/10/31

Weather:cloudy / Wind direction: NE/ Wind force: 4/ Wave: 3 m/ Swell: 3 m/ Visibility: 7nautical miles (12:00 JST)

05:30 Arrival at survey area" F"

05:34 OBEM(LEM03) release command

06:36 OBEM(LEM03) recovery

08:33 XBT

09:00 OBEM(C2) deployment

Transit to survey area" C"

12:46 XBT

13:06 OBEM(C3) deployment

14:45 OBEM(LEM05) release command

17:55 OBEM(LEM05) recovery

18:30-18:40 Scientific meeting

19:20-19:32 Calibration OBEM(C3)

23:05-23:20 Calibration OBEM(C2)

Transit to survey area" E"

2009/11/01

Weather: fine but cloudy / Wind direction: SSW/ Wind force: 7/ Wave: 4 m/ Swell: 3 m/  
Visibility: 6 nautical miles (12:00 JST)

05:30 Arrival at survey area" E"

05:32 OBEM(LEM02) release command

06:44 OBEM(LEM02) recovery

07:46 Pop up HF(PHF01) release command

08:42 Pop-up HF(PHF01) recovery  
09:18 XBT  
09:54-12:47 Heat flow measurement  
13:15 Pop up temperature recorder (PWT01) release command  
13:59 Pop up temperature recorder (PWT01) recovery  
18:00-18:10 Scientific meeting

2009/11/02

Weather: fine but cloudy / Wind direction: NW/ Wind force: 5/ Wave: 3 m/ Swell: 1 m/  
Visibility: 7 nautical miles (12:00 JST)  
05:00 Arrival at survey area" D"  
05:27 OBEM(LEM01) release command  
06:24 OBEM(LEM01) recovery  
06:40 Operation was cancelled due to bad sea condition  
11:50 Arrival at Miyako bay  
18:00-18:30 Scientific meeting

2009/11/03

Weather: fine but cloudy / Wind direction: WNW/ Wind force: 7/ Wave: 5 m/ Swell: 3 m/  
Visibility: 7 nautical miles (12:00 JST)  
08:00 Leave at Miyako bay  
11:50 Arrival at survey area" D"  
12:35 Pop up HF(PHF01) release command  
13:29 Pop-up HF(PHF01) recovery  
13:36 XBT  
14:43-17:08 Heat flow measurement  
18:30-18:40 Scientific meeting  
Transit to survey area" B"

2009/11/04

Weather: fine but cloudy / Wind direction: SW/ Wind force: 6/ Wave: 3 m/ Swell: 3 m/  
Visibility: 7 nautical miles (12:00 JST)  
00:50 Arrival at survey area" B"  
00:55-03:00 MBES survey  
03:43 OBEM(LEM04) release command  
06:49 OBEM(LEM04) recovery  
06:54 XBT  
07:35-11:40 Heat flow + piston core measurement  
12:36-16:30 Heat flow measurement  
18:00-18:10 Scientific meeting

2009/11/05

Weather: fine but cloudy / Wind direction: SW/ Wind force: 5/ Wave: 2 m/ Swell: 1 m/

Visibility: 7 nautical miles (12:00 JST)

07:00 Arrival at Miyako bay

07:58 Get off and onboard

09:30-09:50 Briefing about KAIKO system

11:20 Leave at Miyako bay

15:00 Arrival at survey area" D"

15:45 Pop up temperature recorder (PWT03) release command, no respond

16:30 Stop the collection of PWT03

16:36 Deployment the proton magnetometer

18:00-18:10 Scientific meeting

23:08 Start the geophysical survey

2009/11/06

Weather: fine but cloudy / Wind direction: West/ Wind force: 4/ Wave: 3 m/ Swell: 3 m/

Visibility: 7 nautical miles (12:00 JST)

05:35 Finish the geophysical survey

07:20 Arrival at survey area" A"

07:32 XBT

07:50 Recovery the proton magnetometer

08:11 OBEM deployment

10:35 Launch KAIKO (7K#461dive)

12:51 KAIKO lands (5,215m)

14:03 KAIKO leaves the bottom (5,217m)

16:02 KAIKO on deck

16:40 Deployment the proton magnetometer

17:55-18:20 Scientific meeting

2009/11/07

Weather: fine but cloudy / Wind direction: SSW/ Wind force: 4/ Wave: 2 m/ Swell: 2 m/

Visibility: 7 nautical miles (12:00 JST)

04:15 Finish the geophysical survey

Arrival at survey area" A"

06:59 Recovery the proton magnetometer

08:35 Launch KAIKO (7K#462dive)

10:40 KAIKO lands (5,213m)

12:10 KAIKO leaves the bottom (5,217m)

14:04 KAIKO on deck

13:26 OBEM(A) release command

15:25 OBEM(A) recovery

15:28 Deployment the proton magnetometer  
18:10 Start the geophysical survey  
18:00-18:10 Scientific meeting

2009/11/08

Weather: fine but cloudy / Wind direction: SE/ Wind force: 2/ Wave: 2 m/ Swell: 1 m/

Visibility: 7 nautical miles (12:00 JST)

01:48 Finish the geophysical survey  
06:56 Recovery the proton magnetometer  
07:00 Arrival at survey area" A"  
08:38 Launch KAIKO (7K#463dive)  
12:00 KAIKO lands (5,740m)  
12:51 KAIKO leaves the bottom (5,736m)  
14:56 KAIKO on deck  
14:14 OBEM(C3) release command  
16:31 OBEM(C3) recovery  
16:34 Deployment the proton magnetometer  
17:27 Start the geophysical survey  
18:00-18:10 Scientific meeting

2009/11/09

Weather: fine but cloudy / Wind direction: SW/ Wind force: 5/ Wave: 3 m/ Swell: 2 m/

Visibility: 7 nautical miles (12:00 JST)

02:58 Finish the geophysical survey  
06:30 Recovery the proton magnetometer  
06:33 OBEM(C2) release command  
07:58 OBEM(C2) recovery  
Transit to Kamaishi bay  
14:00 Arrival at Kamaishi bay  
Sheave exchange  
15:00 Transit to survey area "C"  
18:00-18:10 Scientific meeting

2009/11/10

Weather: overcast/ Wind direction: SSW/ Wind force: 2/ Wave: 2 m/ Swell: 2 m/

Visibility: 7 nautical miles (12:00 JST)

06:00 Arrival at survey area" C"  
06:35-10:58 Heat flow + piston core measurement  
10:58 Transit to JAMSTEC  
18:00-18:10 Scientific meeting

2009/11/11

Weather: rain/ Wind direction: NNW/ Wind force: 3/ Wave: 2 m/ Swell: 1 m/

Visibility: 5 nautical miles (12:00 JST)

10:40 Anchor off JAMSTEC

18:00-18:10 Scientific meeting

2009/11/12

09:00 Arrival at JAMSTEC, KR09-16 finish and disembarkation

## 7-2. Bathymetry Survey Lines

Line Name	Start date	Time(UTC)	Latitude	Longitude	End date	Time(UTC)	Latitude	Longitude	Remark
Line1	11/3	15:56	39-02.0251N	144-44.7498E	11/3	18:02	38-58.9484N	145-15.3988E	
Line2	11/5	14:08	39-22.9028N	144-32.8707E	11/5	20:35	39-53.1982N	146-07.5945E	proton magnetmeter
Line3	11/6	09:43	39-52.8852N	146-06.4627E	11/6	14:15	40-13.0236N	147-10.0638E	proton magnetmeter
Line4	11/6	15:05	40-04.3071N	147-07.9332E	11/6	19:16	39-45.4595N	146-11.8711E	proton magnetmeter
Line5	11/7	09:13	39-45.5472N	146-12.1566E	11/7	16:49	39-11.9492N	144-32.8368E	proton magnetmeter
Line6	11/8	08:28	37-59.8539N	144-29.6847E	11/8	12:30	38-15.6522N	145-22.7308E	proton magnetmeter
Line7	11/8	13:27	38-25.2633N	145-23.9766E	11/8	18:00	38-03.9434N	144-19.8035E	proton magnetmeter